

**The Islamic University–Gaza
Research and Postgraduate Affairs
Faculty of Engineering
Master of Electrical Engineering
Control Systems Engineering**



**الجامعة الإسلامية - غزة
شئون البحث العلمي والدراسات العليا
كلية الهندسة
ماجستير الهندسة الكهربائية
هندسة أنظمة تحكم**

Fuzzy Control Design for Quasi-Z-Source Three Phase Inverter

تصميم متحكم ضبابي لدائرة تحويل ذات ثلاثة أطوار من نوع

Quasi-Z-Source

Nouh A. Qaoud

Supervised by

Dr. Basil Hamed

Associate prof. of Control Systems

**A thesis submitted in partial fulfilment
of the requirements for the degree of
Master of Electrical Engineering**

June/2016

إقرار

أنا الموقع أدناه مقدم الرسالة التي تحمل العنوان:

Fuzzy Control Design for Quasi-Z-Source Three Phase Inverter

تصميم متحكم ضبابي لدائرة تحويل ذات ثلاثة أطوار من نوع

Quasi-Z-Source

أقر بأن ما اشتملت عليه هذه الرسالة إنما هو نتاج جهدي الخاص، باستثناء ما تمت الإشارة إليه حيثما ورد، وأن هذه الرسالة ككل أو أي جزء منها لم يقدم من قبل الآخرين لنيل درجة أو لقب علمي أو بحثي لدى أي مؤسسة تعليمية أو بحثية أخرى.

Declaration

I understand the nature of plagiarism, and I am aware of the University's policy on this.

The work provided in this thesis, unless otherwise referenced, is the researcher's own work, and has not been submitted by others elsewhere for any other degree or qualification.

Student's name:	نوح علي قاعود	اسم الطالب:
Signature:		التوقيع:
Date:	15/6/2016	التاريخ:



مكتب نائب الرئيس للبحث العلمي والدراسات العليا هاتف داخلي 1150

الرقم... ج.س.ع/35/..... Ref

2016/08/02

التاريخ..... Date

نتيجة الحكم على أطروحة ماجستير

بناءً على موافقة شئون البحث العلمي والدراسات العليا بالجامعة الإسلامية بغزة على تشكيل لجنة الحكم على أطروحة الباحث/ نوح على نوح قاعود لنيل درجة الماجستير في كلية الهندسة قسم الهندسة الكهربائية - أنظمة التحكم وموضوعها:

تصميم متحكم ضبابي لدائرة تحويل ذات ثلاثة أطوار من نوع Quasi-Z-Source

Fuzzy Control Design for Quasi-Z-Source Three Phase Inverter

وبعد المناقشة العلنية التي تمت اليوم الثلاثاء 14 شوال 1437هـ، الموافق 2016/07/19 م الساعة الحادية عشر صباحاً في قاعة المؤتمرات بمبنى طيبة، اجتمعت لجنة الحكم على الأطروحة والمكونة من:

د. باسل محمود حمد	مشرفاً و رئيساً
د. أسعد نمر أبو جاسر	مناقشاً داخلياً
د. محمد حاتم مشتهى	مناقشاً خارجياً

وبعد المداولة أوصت اللجنة بمنح الباحث درجة الماجستير في كلية الهندسة / قسم الهندسة الكهربائية -

أنظمة التحكم.

واللجنة إذ تمنحه هذه الدرجة فإنها توصيه بتقوى الله ولزوم طاعته وأن يسخر علمه في خدمة دينه ووطنه.

والله والتوفيق ،،،

نائب الرئيس لشئون البحث العلمي والدراسات العليا

أ.د. عبدالرؤف علي المناعمة



DEDICATION

I dedicate this thesis to my father, my wife and my little kid Ali in recognition of their endless help and support; I also dedicate this work to my lovely brothers and sisters.

ACKNOWLEDGEMENT

From the first to the End, I thank ALLAH for giving me the ability to let this thesis finished perfectly. I thank my supervisor Dr. Eng. Basil Hamed for his hard work, helpful suggestions, perfect ideas and advice during this thesis.

I also thank all the team in PCIT for technical experience I get with them, which enable me to complete this thesis in academic field.

Words will not be enough to thank my father and wife for their patience and encouragement during my thesis.

Abstract

Inverters are used widely nowadays because of many of renewable energy source available. These energy source can provide DC voltage like solar panels and the real need of storage energy devices as batteries which also provide DC voltage.

Traditional DC-AC inverters have main limitation, this limitation is that AC output voltage is limited below and cannot exceed the DC-rail voltage. To overcome this limitation and usage of transformer for boosting; in this thesis I explained briefly the Z-source network technique in inverters which can work buck/boost and inverting in one stage without needing to boost DC firstly and then invert or use the same DC to invert and then use transformer to boost.

Later Quasi-Z-Source network was developed, to operate better than Z-Source inverter by lower component ratings, reduced voltage stress, reduced component count and simplified control strategies.

It is common that the M (*Modulation index*) plays the unique effector in controlling Quasi-Z-Source inverters and D_o (*Shoot through duty cycle*) is related to M ; this thesis separates M & D_o as each of them is output control signal of controller. This step added more limitation to component rating because of reducing the current in inductors to half.

Fuzzy Logic control used as a controller for the inverter. This thesis used mamdani method with 3 VDC, IDC and Vc1 input and 2 outputs M and D_o , and centroid method of defuzzification was used. The designed inverter in this thesis could keep the output voltage 208 AC rms 60 Hz with wide range of variable DC input (200-400) v DC.

ملخص الدراسة

تستخدم العواكس الكهربية في الوقت الحاضر على نطاق واسع بسبب تعدد مصادر الطاقة المتجددة المتاحة. ويمكن لمصادر الطاقة هذه توفير تيار كهربي مستمر مثل الألواح الشمسية التي هي في حاجة حقيقية لأجهزة تخزين طاقة مثل البطاريات التي توفر أيضاً تياراً كهربياً مستمراً.

و لعواكس التيار الكهربي التقليدية بعض العيوب و المحددات الرئيسية منها ان التيار المتردد الخارج عنها لا يمكن له أن يتجاوز جهد دي سي-ريل . و للتغلب على هذا القيد، و على استخدام المحولات للتقوية فإنني في هذه الأطروحة اشرح بإيجاز تقنية شبكة مصادر Z في العواكس الكهربية التي يمكن أن تعمل كمحول عكسي لفرق الجهد في أن واحدة دون الحاجة إلى تعزيز التيار المستمر أولاً ثم عكسه أو عكس نفس التيار المستمر أولاً ثم استخدام محول للتقوية.

وبعد ان تم تطوير شبيهه شبكة مصادر Z لتعمل بشكل افضل من تقنية شبكة مصادر Z في العواكس الكهربية من حيث انخفاض في الفلطة المقننة، وانخفاض إجهاد التيار، وانخفاض في عدد المكونات استراتيجيات تحكم ايسط.

من المعروف ان دليل الضمنية (Modulation index) يلعب دوراً مؤثراً في التحكم بشبكات مصادر Z و ان طريقة التحكم المعروفة ب DO (شوت ثرو ديوتي سايكل) مرتبطة بدليل الضمنية. تفصل هذه الأطروحة بين الطريقتين (دليل الضمنية و شوت ثرو ديوتي سايكل) حيث أن كل منهما هو إشارة مراقبة من وحدة تحكم.

تستخدم طريقة تحكم المنطق المشوش (Fuzzy Logic control) كوحدة تحكم للعواكس الكهربية. تستخدم هذه الأطروحة طريقة ممداني بقم إدخال VDC, IDC and Vcl 3 و خرجين (دليل الضمنية و شوت ثرو ديوتي سايكل) و تم استخدام طريقة سنرويد (المركز الوسطي) عملية إزالة التشويش. العاكس الكهربي المصمم في هذه الأطروحة يمكن له أن ينتج تيار كهربي قيمة الجذر التربيعي لمتوسط المربعات 208 و تردد 60 هيرتز مع نطاق واسع من التيار المستمر للإدخال .D (400-200)

List of Contents

DEDICATION	I
ACKNOWLEDGEMENT	II
Abstract	III
ملخص الدراسة	IV
List of Figures.....	VII
List of Tables.....	IX
List of Appendices.....	X
Chapter 1 Introduction	2
1.1 Background	2
1.2 Motivation.....	2
1.3 Contribution	2
1.4 Literature Review	3
1.5 Methodology	5
1.6 Outline.....	5
Chapter 2 Z-Source Inverter	7
2.1 Introduction.....	7
2.2 Circuit Analysis and Obtainable Output Voltage.....	12
2.3 Third-Harmonic Injection Pulse Width Modulation	14
2.3.1 Overview	14
2.3.2 Calculation of Optimum Distortion	14
2.4 Control Methods for Z-Source Inverter	15
2.4.1 Simple Control.....	15
2.4.2 Maximum Boost Control.....	16
2.4.3 Maximum Constant Boost Control.....	17
2.5 Voltage Stress Comparison of the Control Methods	18
2.6 Maximum Constant Boost Control.....	19
Chapter 3 Quasi-Z-Source Inverter.....	24
3.1 Introduction	24
3.2 Quasi-Z-Source Inverter Design	28
Chapter 4 Quasi-Z-Source Inverter Controller Design	31
4.1 Calculations of M and Do	31
4.2 Fuzzy Controller Memberships	32
4.2.1 Introduction	32
4.2.2 VDC Input	33

4.2.3	IDC Input.....	34
4.2.4	Vc1 Input.....	35
4.2.5	M output.....	36
4.2.6	Do Output.....	37
4.3	Surfaces.....	39
4.4	Simulink Model.....	40
4.5	Results.....	43
Chapter 5 Conclusion and Future Research		46
5.1	Conclusions	46
5.2	Future Work	46
References.....		47
Appendices		49
	Appendix A.....	49

List of Figures

Figure 2.1 Traditional Voltage-Source Inverter	7
Figure 2.2 Z-source inverter	8
Figure 2.3 Traditional signals for square wave.	9
Figure 2.4 PWM Signals for sine wave.....	10
Figure 2.6 Equivalent circuit of Z-Source at one of eight traditional vectors, with I equal zero at two zero states.	11
Figure 2.5 Equivalent circuit of the Z-source inverter viewed from the DC link.	11
Figure 2.5 Equivalent circuit of Z-Source at ninth state or shoot throw state.....	12
Figure 2.6 Modulation Signal with third Harmonic Injection	14
Figure 2.7 Sketch map of simple control	16
Figure 2.8 Maximum boost control.....	16
Figure 2.9 Maximum boost control with third harmonic injection.....	17
Figure 2.13 Maximum constant boost control with third harmonic injection	17
Figure 2.12 Maximum constant boost.....	17
Figure 2.10 Voltage stress comparison	18
Figure 2.11 Voltage gain (MB) versus M	20
Figure 2.12 Voltage gain (MB) versus M in third harmonic injection	22
Figure 3.1 Voltage Fed qZSI with Continuous Input Current	24
Figure 3.2 Voltage Fed qZSI with Discontinuous Input Current	24
Figure 3.3 Equivalent circuit of the qZSI in non-shoot-through states.....	25
Figure 3.4 Equivalent circuit of the qZSI in shoot-through states.....	26
Figure 4.1 Memberships Functions of VDC Input	34
Figure 4.2 Memberships Functions of IDC Input.....	35
Figure 4.3 Memberships Functions of Vc1 Input	36
Figure 4.4 Memberships Functions of M Output	37
Figure 4.5 Memberships Functions of Do Output	38
Figure 4.6 Surface for M Output	39
Figure 4.7 Surface for Do Output	39
Figure 4.8 Simulink Model of all system.....	41
Figure 4.9 Pulses Block.....	42
Figure 4.10 Results of Variable VDC Input (200-400).....	43

Figure 4.11 Result of Fixed Input 200 V DC with fuzzy controller. 44
Figure 4.12 Result of Fixed Input 200 V DC without controller..... 44

List of Tables

Table 3.1 Voltage and average current of the qZSI and ZSI network	27
Table 3.2The main parameters of inverter	28
Table 3.3The parameters of qZSI network.....	29
Table 4.1Samples of VDC.....	32
Table 4.2Memberships of VDC Input.....	33
Table 4.3Memberships of IDC Input	34
Table 4.4Memberships of Vc1 Input	35
Table 4.5Memberships of M Output.....	36
Table 4.6Memberships of Do Output.....	37
Table Appendix. 1 Fuzzy Rules.....	49

List of Appendices

Appendix 1	49
------------------	----

Chapter 1

Introduction

Chapter 1 Introduction

1.1 Background

Converting electrical energy from type to type becomes very important and necessary day by day due to many new renewable energy sources.

One of the most important converting devices is DC-AC inverter. Before 2003, the traditional inverter was the most common, then in 2003, Prof.Fang Zheng Peng published a paper (Peng, MARCH/APRIL 2003) with new technique for inverting named Z-source network (described in chapter 2).

Controlling Z-Source inverter has three methods: simple boost, maximum simple boost and maximum constant boost .each of them has its advantages and disadvantages but in this thesis maximum constant boost was used because of its optimum behaviour for voltage stress and harmonics in output wave.

Then new techniques become improved to achieve the quasi-Z-source with its four methods as described in chapter 3 with Quasi-Z-Source inverter ripple in inductor current was minimized and voltage stress over switches was minimized also.

Fuzzy control system established by Prof Zadeh in 1965 can convert linguistic variables to crisp values. In this thesis fuzzy logic controlled applied to quasi-Z-source inverter and the desired result with variable input DC voltage and fixed output AC voltage was achieved.

1.2 Motivation

Regular electrical energy conversion devices use transformer as main element in device and this costs more money, weight and volume. This point leads researchers to develop new methods to overcome that problem and reduce the number of circuits in one device to one circuit can boost and buck together as z-source and quasi-Z-source networks.

With this new circuit, it was necessary to develop suitable control method, so I used fuzzy controller and simulated the result to get the desired values.

1.3 Contribution

In this thesis a new Fuzzy controller was designed to control Z-source network and its analysis, besides to all effective techniques for improving the output wave shape.

To avoid some of the problems of Z-source inverter like variable current in inductor and high voltage stress, quasi-Z-source was described briefly.

Controlling the inverter was done by fuzzy controller with mamdani method and centroid defuzzification .

1.4 Literature Review

In 2003 Fang Zheng Peng published a paper presents an impedance-source power converter (abbreviated as Z-source converter) and its control method for implementing DC-to-AC, AC-to-DC, AC-to-AC, and DC-to-DC power conversion. The Z-source converter employs a unique impedance network (or circuit) to couple the converter main circuit to the power source, thus providing unique features that cannot be obtained in the traditional converters where a capacitor and inductor are used, respectively. The Z-source converter overcomes the conceptual and theoretical barriers and limitations of the traditional converters and provides a novel power conversion concept. (Peng, MARCH/APRIL 2003)

In 2004 Miaosen Shen, Jin Wang, Alan Joseph, Fang Z. Peng, Leon M. Tolbert, and Donald J. Adams. published a paper called "Maximum Constant Boost Control of the Z-Source Inverter". In this paper Adams. proposes two maximum constant boost control methods for the Z-source inverter, which can obtain maximum voltage gain at any given modulation index without producing any low-frequency ripple that is related to the output frequency. Thus the Z-network requirement will be independent of the output frequency and determined only by the switching frequency. (Shen, et al., 2004)

In 2005 Oak Ridge National Laboratory prepared a project called "Z-Source Inverter for Fuel Cell Vehicles". In this project all the features of Z-Source inverter were discussed especially control methods of Z-source inverter with comparison of advantages and disadvantages of each method. (Ride & Olszewski, 2005)

In 2006 Miaosen Shen, Jin Wang, Fang Zheng Peng, Leon M. Tolbert and Donald J. Adams. Published a paper called "Constant Boost Control of the Z-Source Inverter to Minimize Current Ripple and Voltage Stress". This paper proposes two constant boost-control methods for the Z-source inverter, which can obtain maximum voltage gain at any given modulation index without producing any low-frequency ripple that is related to the output frequency and minimize the voltage stress at the same time. Thus, the Z-network requirement will be independent of the output frequency and determined only by the switching frequency. (Shen, Wang, Peng, Tolbert, & Adams, 2006)

In 2008 J. Anderson, F.Z. Peng, published a paper called "Four Quasi-Z-Source Inverters". In this paper, theoretical results are shown for several novel inverters. These inverters are similar to the Z-source inverters presented in previous works, but have several advantages, including in some combination; lower component ratings, reduced source stress, reduced component count and simplified control strategies. Like the Z-Source inverter, these inverters are particularly suited for applications which require a large range of gain, such as in motor controllers or renewable energy. (Anderson & Peng, 2008)

In 2009 Y. Li, J. Anderson, F. Z. Peng, and D. C. Liu. published a paper called “Quasi-Z-source inverter for photovoltaic power generation systems” . This paper presents a quasi-Z-source inverter (qZSI) that is a new topology derived from the traditional Z-source inverter (ZSI). The qZSI inherits all the advantages of the ZSI, which can realize buck/boost, inversion and power conditioning in a single stage with improved reliability. In addition, the proposed qZSI has the unique advantages of lower component ratings and constant DC current from the source. All of the boost control methods that have been developed for the ZSI can be used by the qZSI. (Li, Anderson, Peng, & Liu, 2009)

In 2012 Pranay S.Shete,Rohit G. Kanojiya and Nirajkumer S.Maurya published a paper called “Performance of Sinusoidal Pulse Width Modulation based Three Phase Inverter”. In this paper a new sinusoidal PWM inverter suitable for use with power MOSFETs is described. . The output waveforms in the proposed PWM inverter are investigated both theoretically and experimentally. The fundamental component of the three-phase line-to-line voltage is increased by about 15 percent above than that of the conventional sine-wave inverter. (Shete, Kanojiya, & Maurya, 2012)

In 2012 Penchalababu.V, Chandrakala.B and Gopal Krishna published a paper called “A Survey on Modified PWM Techniques for Z-Source Inverter”. In this proposed work presents controlling the shoot-through duty cycle of IGBTs in inverter system, reducing the line harmonics, improving power factor, and extending output voltage range. This Paper presents different switching techniques such as Simple boost pwm, Constant boost pwm, Maximum boost pwm, Sine carrier pwm and Modified SVPWM. (Penchalababu, Chandarakala, & Karismna, 2012)

In 2013 Prachi S.Dharmadhikar published a paper which was comparative analysis of the carrier based pulse width with third harmonic injection and Digital pulse Width used in the inverter control is presented. The placement of the modulating components within the carrier interval determines the harmonic performance of the modulation strategy. The third harmonic injected modulated inverter and the digital pulse width modulation technique gives higher value of line to line voltage as compared with the conventional sine pulse width modulated (SPWM) inverter. The optimized third-harmonic injection controls the blanking time and minimum pulse width of an operating inverter switch. (Dharmadhikari, 2013)

In 2013 Budi Yanto Husodo, Shahrin Md. Ayob and Makbul Anwari, Taufik. Ppublished a paper called ” Simulation of Modified Simple Boost Control for Z-Source Inverter” In this paper, a simple boost control with independence relation between modulation index and shoot-through duty ratio (modified simple boost) for z-source inverter is simulated and analysed using MATLAB/Simulink, as well as the simple boost and the maximum boost control methods. (Husodo, Ayoub, Anwari, & Taufik, 2013)

In 2013 S.Sathya, C.karthikeyan. published a paper called” Fuzzy Logic Based Z-Source Inverter for Hybrid Energy Resources” This paper proposes a fuzzy logic based voltage controller for hybrid energy resources using Z-source inverter. (Sathya & Karthikeyan, 2013)

In 2013 Yuan Li, Shuai Jiang, Jorge G. Cintron-Rivera, and Fang Zheng Peng, polished a paper called “Modelling and Control of Quasi-Z-Source Inverter for Distributed Generation Applications” This paper further addresses detailed modelling and control issues of the qZSI used for distributed generation (DG), such as PV or fuel cell power conditioning. The dynamical characteristics of the qZSI network are first investigated by small-signal analysis. Based on the dynamic model, stand-alone operation and grid-connected operation with closed-loop control methods are carried out, which are the two necessary operation modes of DG in distributed power grids. Due to the mutual limitation between the modulation index and shoot-through duty ratio of qZSI, constant capacitor voltage control method is proposed in a two-stage control manner. Minimum switching stress on devices can be achieved by choosing a proper capacitor voltage reference. (Li, Jiang, Cintron-Rivera, & Peng, 2013)

In 2013 Baoming Ge, Haitham Abu-Rub, Fang Zheng Peng, Qin Lei, Anibal T. de Almeida, Fernando J. T. E. Ferreira, Dongsun Sunand Yushan Liu, published a paper called “ An Energy-Stored Quasi-Z-Source Inverter for Application to Photovoltaic Power System” in this paper discussed The quasi-Z-source inverter (qZSI) with battery operation and its ability to balance the stochastic fluctuations of photovoltaic (PV) power injected to the grid/load, but its existing topology has a power limitation due to the wide range of discontinuous conduction mode during battery discharge. This paper proposes a new topology of the energy-stored qZSI to overcome this disadvantage. (Ge, et al., 2013)

1.5 Methodology

To reach this aim, inverters will be studied perfectly to decide which technique is the best for my application, then parameters for the inverter will be chosen. Finally a fuzzy controller will be designed to finish the inverter.

1.6 Outline

This thesis is organized into five chapters. Chapter 1 introduce this thesis and Chapter 2 handles principles of 3 phase regular inverters and the analysis of z-source inverter .Chapter 3 handles briefly quasi-Z-source and system design. Chapter 4 presents the design of fuzzy controller and the results. The last chapter concludes the design and implementation and proposes some future work.

Chapter 2

Z-Source Inverter

Chapter 2 Z-Source Inverter

2.1 Introduction

There is a traditional voltage-source inverter as in fig (2.1), which is supported by DC source. The DC voltage source can be a battery, fuel-cell stack, diode rectifier, and/or capacitor. Six switches are used in the main circuit; each is traditionally composed of a power transistor and an antiparallel (or freewheeling) diode to provide bidirectional current flow and unidirectional voltage blocking capability.

The AC output voltage is limited below the DC-rail voltage. Therefore, the V-source inverter is a buck (step-down) inverter for DC-to-AC power conversion. For applications where over drive is desirable and the available DC voltage is limited, an additional DC-DC boost converter is needed to obtain a desired AC output. The additional DC-DC boost converter stage increases system cost and lowers efficiency.

The upper and lower switches of each phase leg cannot be gated on simultaneously. Otherwise shoot-through (i.e., a state occurs when two switches at the same leg are turned on) would occur and destroy the devices.

An output *LC* filter is needed for providing a sinusoidal voltage, which causes additional power loss due to the small but non-zero resistance within the components and connecting wires.

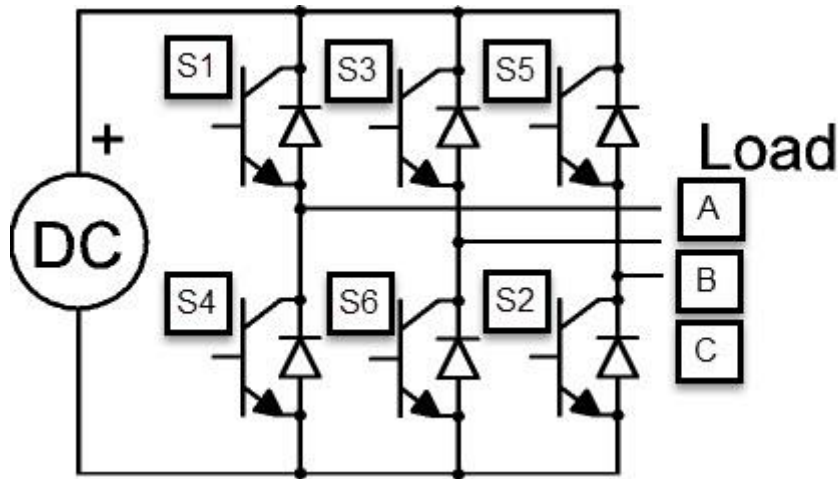


Figure 2.1 Traditional Voltage-Source Inverter

To overcome the previous problems of the traditional V-source inverters, an impedance-source power converter (abbreviated as Z-source inverter) was developed as in Fig. 2.2 which shows the general Z-source inverter structure. It employs a unique impedance network (or circuit) to couple the inverter main circuit to the power source, load, or other converter to provide unique features that cannot be observed in the traditional V- source inverters where a capacitor and inductor are used respectively. The Z-source inverter overcomes the above-mentioned concept and theoretical barriers and limitations of the traditional V-source inverter and also provides a novel power conversion concept.

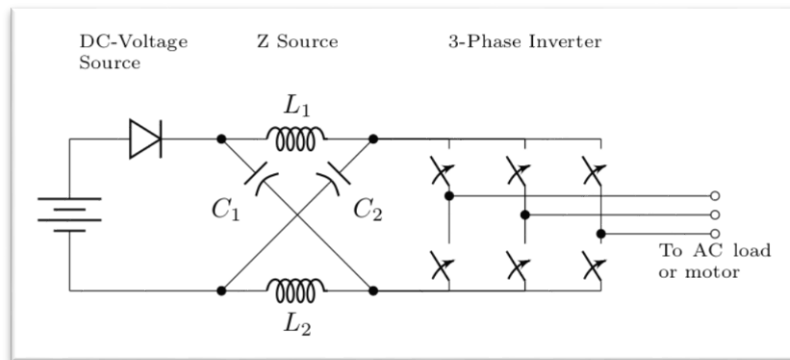


Figure 2.2 Z-source inverter

In Fig. 2.2, a diode is located between a DC source and a two-port network to prevent DC source from the high network voltage. The two-port network that consists of a split-inductor L_1 and L_2 and capacitors C_1 and C_2 connected in X shape is employed to provide an impedance source (Z-source) coupling the converter (or inverter) to the DC source, load, or another converter. The DC source/or load can be either a voltage or a current source/or load. Therefore, the DC source can be a battery, diode rectifier, thyristor converter, fuel cell, an inductor, a capacitor, or a combination of those. Switches used in the converter can be a combination of switching devices and diodes such as the antiparallel combination as shown in Fig. 2.1, the Z-source concept can be applied to all DC-to-AC, AC-to-DC, AC-to-AC, and DC-to-DC power conversion.

The unique feature of the Z-source inverter is that the output AC voltage can be any value between zero and infinity regardless of the fuel-cell voltage. That is, the Z-source inverter is a Buck–Boost inverter that has a wide range of obtainable voltage. The traditional V- inverters cannot provide such feature.

To describe the operating principle and control of the Z-source inverter in Fig. 2.2, let us briefly examine the Z-source inverter structure. In Fig. 2.2, the three-phase Z-source inverter bridge has nine permissible switching states (vectors) unlike the traditional three-phase V-source inverter that has eight. The traditional three-phase V-source inverter has six active vectors, when the DC voltage is impressed across the load and two zero vectors when the load terminals are shorted through either the lower or upper three devices, respectively. However, the three-phase Z-source inverter bridge has one extra zero state.

This new extra zero state occurs when the load terminals are shorted through both the upper and lower devices of any one phase leg (i.e., both devices are gated on), any two phase legs, or all three phase legs. This shoot-through zero state (or vector) is forbidden in the traditional V-source inverter, because it would cause a shoot-through. We call this third zero state (vector) the shoot-through zero state (or vector), which can be generated by seven different ways: shoot-through via any one phase leg, combinations of any two phase legs, and all three phase legs. The Z-source network makes the shoot-through zero state possible. This shoot-through zero state provides the unique buck-boost feature to the inverter. (Peng, MARCH/APRIL 2003)

The six active vectors for traditional inverter are described in Fig2.3 and Fig2.4 for square wave and sine wave respectively.

The new extra zero state have 7 statuses could occur with, all these statuses and traditional eight are described in table .2.1

The equivalent circuit of the Z-source inverter as shown in Fig. 2.2 will be as Fig 2.5 when viewed from the DC link. The inverter bridge is equivalent to a short circuit when the inverter bridge is in the shoot-through zero state, as shown in Fig. 2.7, whereas the inverter bridge becomes an equivalent current source as shown in Fig. 2.6 when in one of the six active states. Note that the inverter bridge can be also represented by a current source with zero value (i.e., an open circuit) when it is in one of the two traditional zero states.

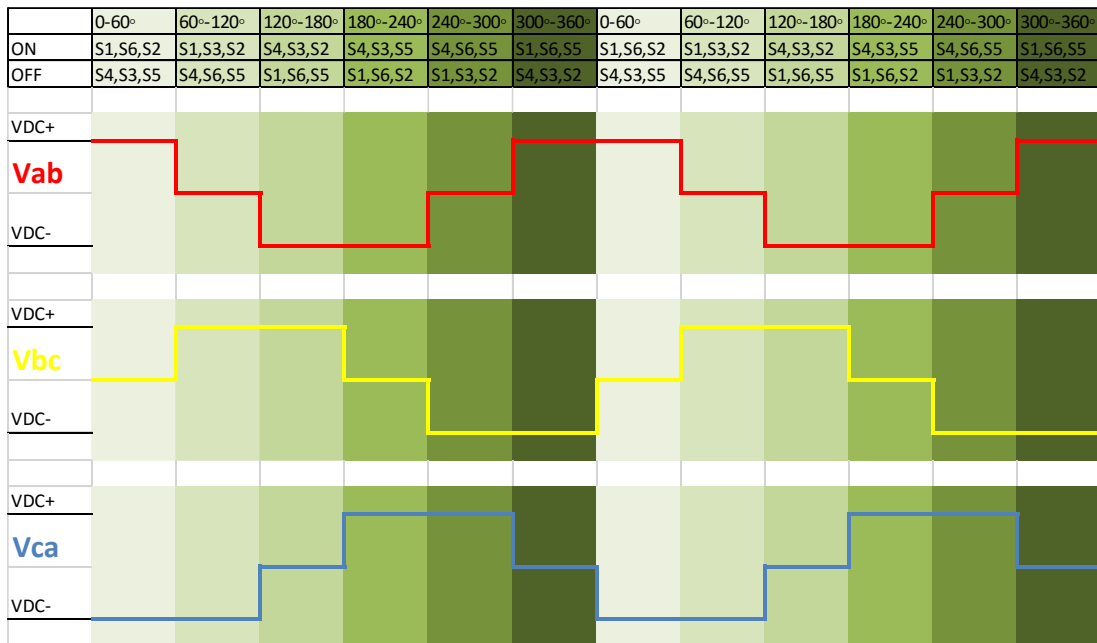


Figure 2.3 Traditional signals for square wave.

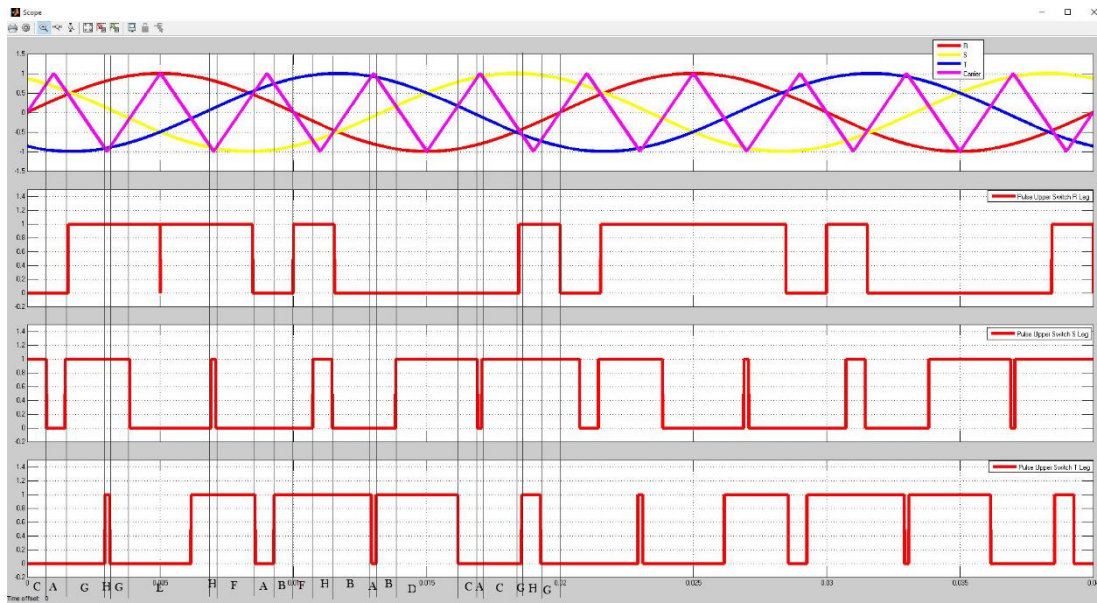


Figure 2.4 PWM Signals for sine wave

Table 2.1 Statuses and switches conditions

Active Vectors	On	Off
E	S1,S6,S2	S4,S3,S5
G	S1,S3,S2	S4,S6,S5
C	S4,S3,S2	S1,S6,S5
D	S4,S3,S5	S1,S6,S2
B	S4,S6,S5	S1,S3,S2
F	S1,S6,S5	S4,S3,S2
Zero Vectors	On	Off
A	S4,S6,S2	S1,S3,S5
H	S1,S3,S5	S4,S6,S2

Extra Zero Vectors	On	Regardless of which of other switches are off
Z	S1,S4	I
Z	S3,S6	II
Z	S5,S2	III
Z	S1,S4,S3,S6	IV
Z	S1,S4,S5,S2	V
Z	S3,S6,S5,S2	VI
Z	S1,S4,S3,S6,S5,S2	VII

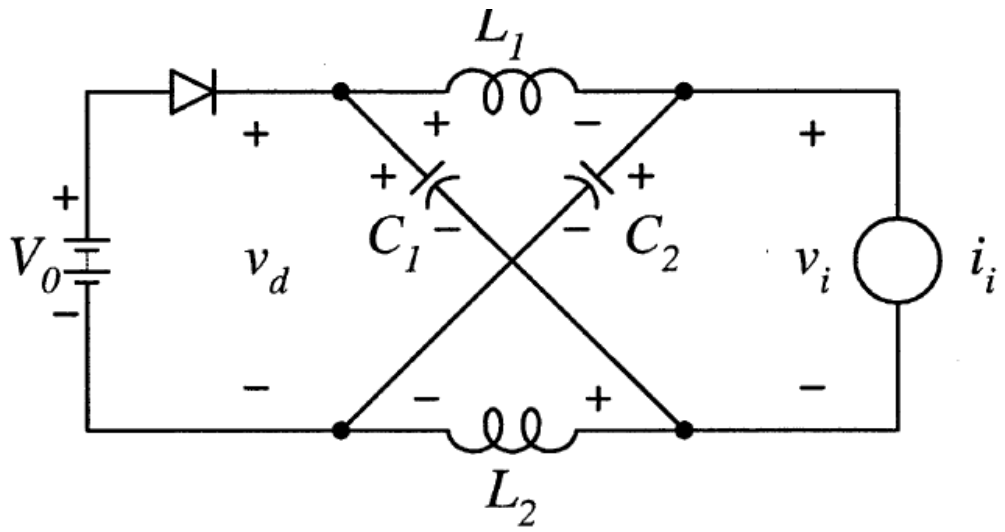


Figure 2.5 Equivalent circuit of the Z-source inverter viewed from the DC link.

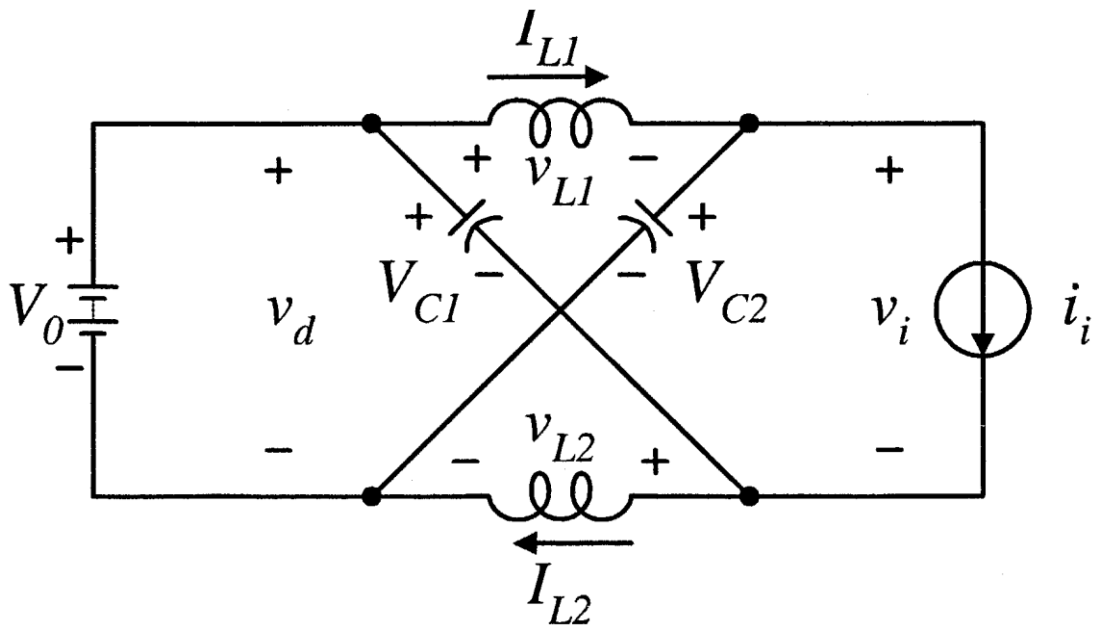


Figure 2.6 Equivalent circuit of Z-Source at one of eight traditional vectors, with I equal zero at two zero states.

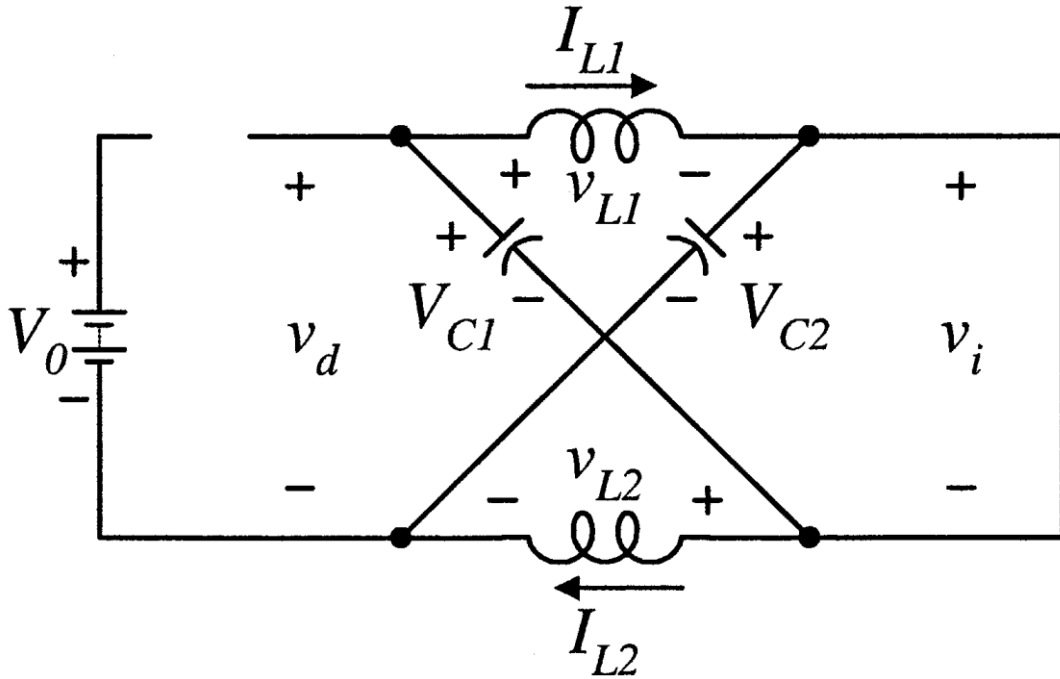


Figure 2.5 Equivalent circuit of Z-Source at ninth state or shoot throw state

2.2 Circuit Analysis and Obtainable Output Voltage

Assuming that the inductors L_1 and L_2 and capacitors C_1 and C_2 have the same inductance and capacitance, respectively, the Z-source network becomes symmetrical. From the symmetry and the equivalent circuits, we have

$$V_{C1} = V_{C2} = V_C \quad V_{L1} = V_{L2} = V_L \quad (2.1)$$

Given that the inverter bridge is in the shoot-through zero state for an interval of T_0 , during a switching cycle T , and from the equivalent circuit, Fig. 2.7

$$V_L = V_C \quad V_D = V_C + V_L \quad V_D = 2V_C \quad V_i = 0 \quad (2.2)$$

Now consider that the inverter bridge is in one of the eight nonshoot-through states for an interval of T_1 , during the switching cycle T , from the equivalent circuit, Fig. 2.6,

$$V_L = V_0 - V_C \quad V_D = V_0 \quad V_i = V_C - V_L = 2V_C - V_0 \quad (2.3)$$

Where V_0 is the DC source voltage and $T = T_0 + T_1$.

The average voltage of the inductors over one switching period T should be zero in steady state, from (2.2) and (2.3), thus, we have

$$V_l = \frac{T_o * V_c + T1 * (V_o - V_c)}{T} \quad (2.4)$$

$$\text{Or } \frac{V_c}{V_o} = \frac{T1}{T1 - T_o} \quad (2.5)$$

Similarly, the average DC-link voltage across the inverter bridge can be found as follows:

$$\bar{v}_i = \frac{T_o * 0 + T1 * (2V_c - V_o)}{T} = \frac{T1}{T1 - T_o} V_o = V_c \quad (2.6)$$

The peak DC-link voltage across the inverter bridge is expressed in (2.3) and can be rewritten as:

$$\bar{v}_i = V_c - v_l = 2V_c - V_o = \frac{T}{T1 - T_o} V_o = B * V_o \quad (2.7)$$

$$\text{Where: } B = \frac{T}{T1 - T_o} = \frac{1}{1 - 2 \frac{T_o}{T}} \geq 1 \quad (2.8)$$

B is the boost factor resulting from the shoot-through zero state. The maximum B (infinity) occurs when T_o equals $T1$, but the minimum value of B (1) occurs when T_o equals Zero.

The peak DC-link voltage \bar{v}_i is the equivalent DC-link voltage of the inverter. On the other side, the output peak phase voltage from the inverter can be expressed as:

$$\hat{V}_{ac} = M * \frac{\hat{V}_i}{2} \quad (2.9)$$

Where M is the modulation index:

The maximum value of M equals 1 which means the peak of AC output equals half of DC. The lower the value of M is, the lower the value of the peak of AC is.

Using (2.7), (2.9) can be further expressed as:

$$\hat{V}_{ac} = M * B * \frac{V_o}{2} \quad (2.10)$$

The buck–boost factor $M.B$ is determined by the modulation index M and the boost factor B . The boost factor B as expressed in (2.8) can be controlled by duty cycle of the shoot-through zero state over the nonshoot-through states of the inverter PWM.

Notice that the shoot-through zero state does not affect the PWM control of the inverter, because it equivalently produce the same zero voltage to the load terminal. The available shoot-through period is limited by the zero-state period that is determined by the modulation index. (Peng, MARCH/APRIL 2003)

2.3 Third-Harmonic Injection Pulse Width Modulation

2.3.1 Overview

The third – harmonic PWM is similar to the selected harmonic injection method & it is implemented in the same manner as sinusoidal PWM. The difference is that the reference AC waveform is not sinusoidal but consists of both a fundamental component and a third-harmonic component. As a result, the peak-to-peak amplitude of the resulting reference function does not exceed the DC supply voltage V_s , but the fundamental component is higher than the available supply V_s . The reference voltage V_{ref} is added with signal having frequency three times of fundamental frequency and the magnitude is $1/6$ th of the fundamental amplitude. The resultant is then passed through comparator which compares the modified signal with the carrier.

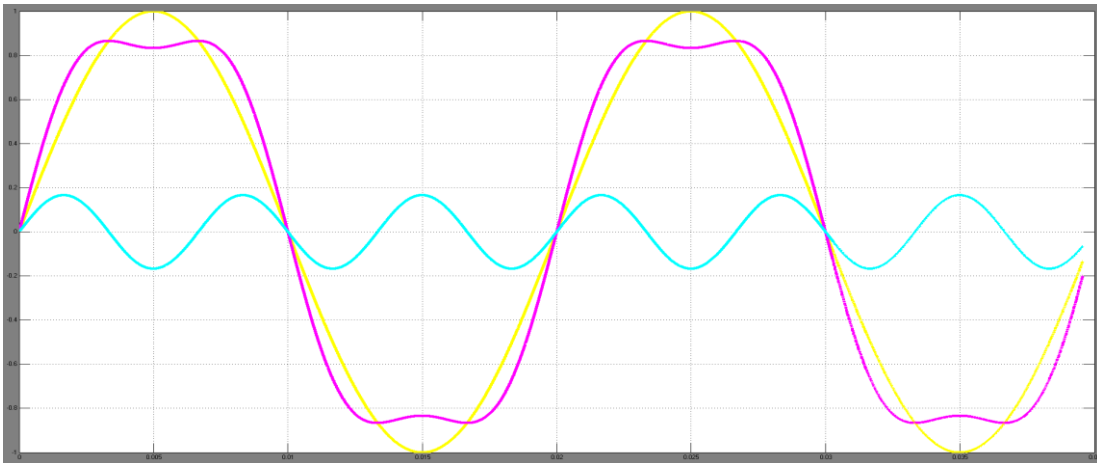


Figure 2.6 Modulation Signal with third Harmonic Injection

The presence of exactly the same third-harmonic component in each phase results in an effective cancellation of the third harmonic component in the neutral terminal, and the line-to-neutral phase voltages are all sinusoidal with the peak amplitude. By injecting the third harmonic into the reference voltage signal, the fundamental of the phase voltage can be increased. The voltage can be increased by harmonic suppression for the rectifiers as well as inverters. This can be mainly done by injecting the third harmonic.

2.3.2 Calculation of Optimum Distortion

The generation of the phase voltage waveform having no third harmonics can be generated by addition of the third harmonics in the sinusoidal reference waveform. These additions of the various amounts of third, ninth, fifteenth etc. harmonics is used to produce flat-topped phase waveforms which improves the efficiency of the inverters. The optimal amount of third harmonic should extend the ratings of all PWM inverters. The best modification that can be made to the inverter phase output

waveform is assumed a priori to be the addition of a measure of third harmonics. The desired waveform of the type

$$y = \sin \omega t + A \sin 3\omega t \quad (2.11)$$

Where A is to be determined for the optimal of Y. The optimal injection is obtained by differentiating (2.11)

$$\frac{dy}{dt} = \cos \omega t + A \cos 3\omega t = 0 \quad (2.12)$$

The maxima and minima of the waveform therefore occur at

$$\cos \omega t = 0 \quad \text{and} \quad \cos \omega t = \left(\frac{9A-1}{12A} \right)^{1/2} \quad (2.13)$$

$$\sin \omega t = 0 \quad \text{and} \quad \sin \omega t = \left(\frac{1+3A}{12A} \right)^{1/2} \quad (2.14)$$

Manipulating the (11) using identity, we get

$$y = (1+3A)\sin \theta - 4A \sin^3 \theta \quad (2.15)$$

Substituting the values of sin θ obtained, we get

$$\hat{y} = 1 - A \quad \text{and} \quad \hat{y} = 8A \left(\frac{1+3A}{12A} \right)^{3/2} \quad (2.16)$$

The optimum value of A is that value which minimizes \hat{y} and can be found by differentiating the expression for \hat{y} and equating it to zero. Thus the values of A are

$$A = \frac{-1}{3} \quad \text{and} \quad A = \frac{1}{6}$$

The value of \hat{y} cannot be greater than unity for this reason the value $A = -1/3$ is discarded. The required value of A is therefore 1/6, and the required waveform is

$$u = \sin \theta + \frac{1}{6} \sin 3\theta \quad (2.17)$$

So the relation 2.17 describes the third harmonic injection. (Dharmadhikari, 2013)

2.4 Control Methods for Z-Source Inverter

2.4.1 Simple Control

The simple control uses two straight lines to control the shoot-through states, as shown in Fig. 2.9. When the triangular waveform is greater than the upper envelope, V_p , or lower than the bottom envelope, V_n , the circuit turns into shoot-through state. Otherwise it operates just as traditional carrier-based PWM. This method is very

straightforward; however, the resulting voltage stress across the device is relatively high because some traditional zero states are not utilized.

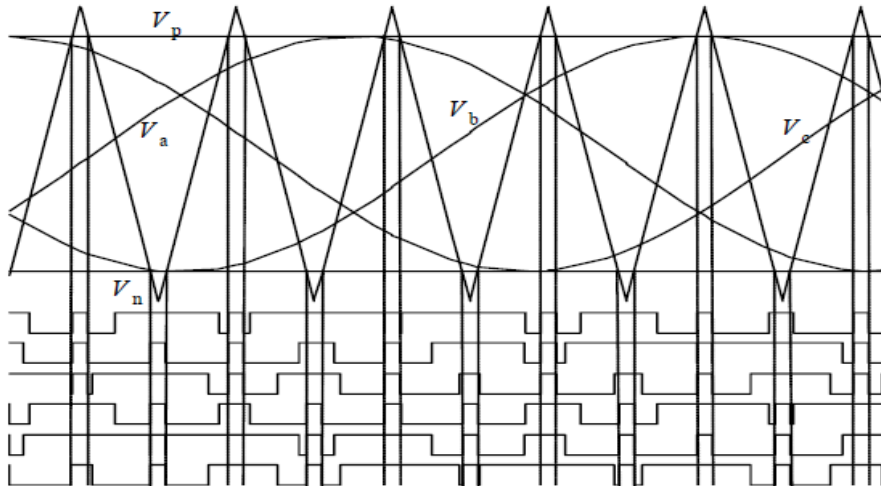


Figure 2.7 Sketch map of simple control

2.4.2 Maximum Boost Control

To fully utilize the zero states so as to minimize the voltage stress across the device, maximum boost control turns all traditional zero states into shoot-through state, as shown in Fig. 2.10 Third harmonic injection can also be used to extend the modulation index range. Indeed, turning all zero states into shoot-through state can minimize the voltage stress; however, doing so also causes a shoot-through duty ratio varying in a line cycle, which causes inductor current ripple. This will require high inductance for low-frequency or variable-frequency applications.

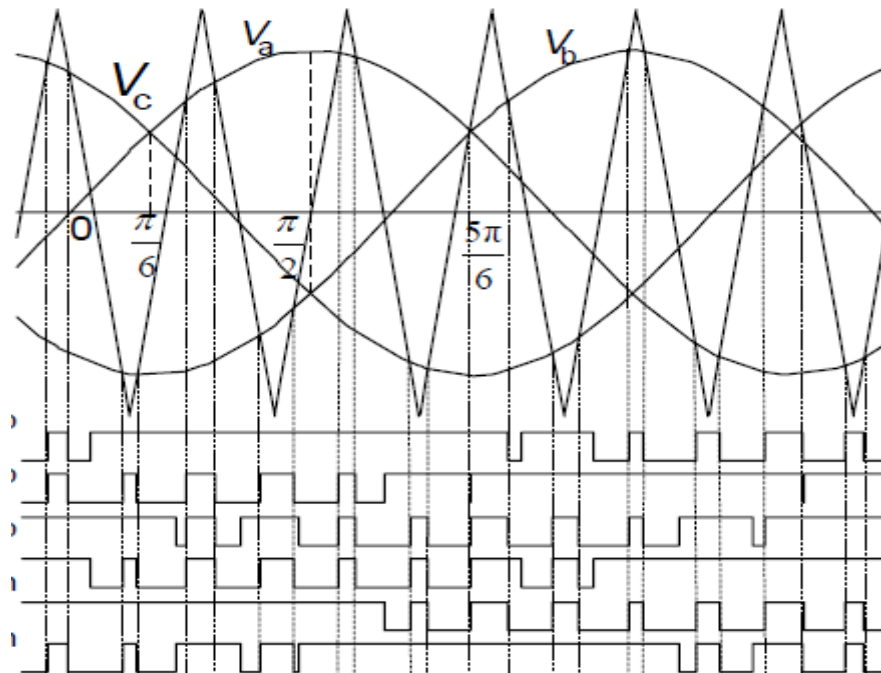


Figure 2.8 Maximum boost control

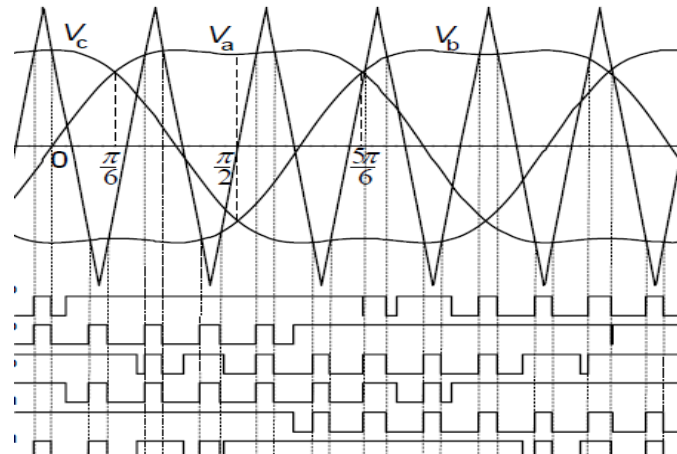


Figure 2.9 Maximum boost control with third harmonic injection

2.4.3 Maximum Constant Boost Control

The sketch map of maximum constant boost control is shown in Fig. 2.12, this method achieves maximum boost while keeping the shoot-through duty ratio always constant; thus it results in no line frequency current ripple through the inductors. The sketch map of maximum constant boost control with third harmonic injection is shown in Fig.2.13. With this method, the inverter can buck and boost the voltage from zero to any desired value smoothly within the limit of the device voltage. (Ride & Olszewski, 2005)

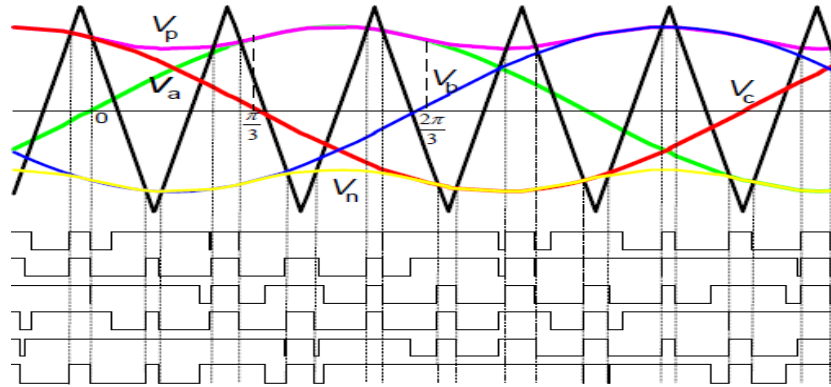


Figure 2.12 Maximum constant boost

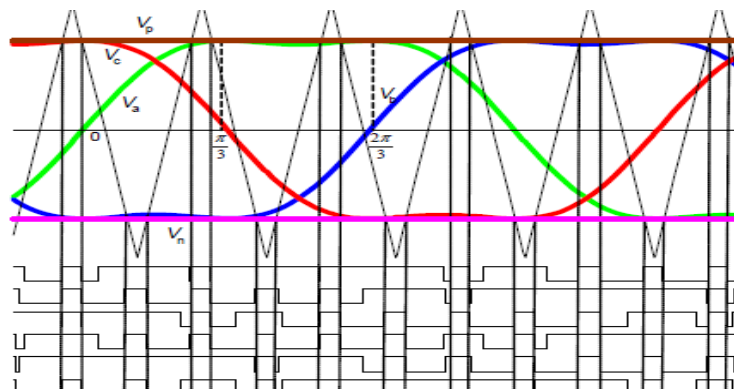


Figure 2.13 Maximum constant boost control with third harmonic injection

2.5 Voltage Stress Comparison of the Control Methods

To examine the voltage stress across the switching devices, an equivalent DC voltage is introduced. The equivalent DC voltage is defined as the minimum DC voltage needed for the traditional voltage-source inverter to produce the same output voltage. The ratio of the voltage stress to the equivalent DC voltage represents the cost that Z-source inverter has to pay to achieve voltage boost.

The ratios of the voltage stress to the equivalent DC voltage, $kstress$, for the simple control, maximum boost control, and maximum constant boost control are summarized as follows:

$$Kstress = 2 - \frac{1}{G} \text{ for simple control} \quad (2.18)$$

$$Kstress = \frac{3\sqrt{3}}{\pi} - \frac{1}{G} \text{ for maximum boost} \quad (2.19)$$

$$Kstress = \sqrt{3} - \frac{1}{G} \text{ for maximum constant boost} \quad (2.20)$$

where G is the voltage gain defined as

$$G = M \bullet B = \frac{\bar{V}_{AC}}{V_{dc}/2} \quad (2.21)$$

Where \bar{V}_{AC} is the peak output phase voltage and V_{DC} is the input voltage to the Z-source inverter. The comparison is shown in Fig.2. 14. In the figure, the voltage stress of simple control is highest among the three, and the maximum boost achieves the minimum voltage stress. However, the maximum boost suffers from the six time load frequency current ripple through the inductor;

Therefore, the maximum constant boost control is the most suitable method for our application. Also, the maximum constant boost with third harmonic injection seems to be the better one because it can achieve continuous output voltage variation from zero to infinity. (Ride & Olszewski, 2005)

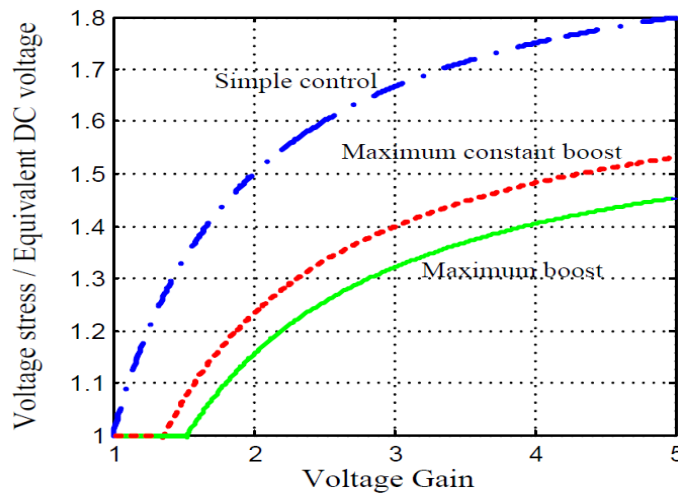


Figure 2.10 Voltage stress comparison

2.6 Maximum Constant Boost Control

In order to reduce the volume and cost of the Z-source network, we need to eliminate the low-frequency current ripple by using a constant shoot-through duty ratio. At the same time, a greater voltage boost for any given modulation index is desired to reduce the voltage stress across the switches. Fig11.a shows the sketch map of the maximum constant boost control method, which achieves the maximum voltage gain while always keeping the shoot-through duty ratio constant. There are five modulation curves in this control method: three reference signals V_a, V_b and V_c and two shoot-through envelope signals V_p and V_n . When the carrier triangle wave is higher than the upper shoot-through envelope V_p or lower than the bottom shoot-through envelope V_n the inverter is turned to a shoot-through zero state. In between, the inverter switches in the same way as in the traditional carrier based PWM control. Because the boost factor is determined by the shoot-through duty cycle, the shoot-through duty cycle must be kept the same from switching cycle to switching cycle in order to maintain a constant boost. The basic point is to get the maximum B while keeping it constant all the time. The upper and lower envelope curves are periodical and are three times the output frequency. There are two half-periods for both curves in a cycle. For the first half-period, $[0, \pi/3]$ in Fig12, the upper and lower envelope curves can be expressed by (2.22) and (2.23), respectively

$$V_{p1} = \sqrt{3}M + \sin(\theta - \frac{2\pi}{3})M \quad 0 < \theta < \frac{\pi}{3} \quad (2.22)$$

$$V_{n1} = \sin(\theta - \frac{2\pi}{3})M \quad 0 < \theta < \frac{\pi}{3} \quad (2.23)$$

For the second half-period $[\pi/3, 2\pi/3]$, the envelope curves are expressed by (2.24) and (2.25), respectively

$$V_{p2} = \sin(\theta)M \quad \frac{\pi}{3} < \theta < \frac{2\pi}{3} \quad (2.24)$$

$$V_{n2} = \sin(\theta)M - \sqrt{3}M \quad \frac{\pi}{3} < \theta < \frac{2\pi}{3} \quad (2.25)$$

Obviously, the distance between these two curves determining the shoot-through duty ratio is always constant for a given modulation index M , that is, $\sqrt{3}M$. Therefore, the shoot through duty ratio is constant and can be expressed as :

$$\frac{T_o}{T} = \frac{2 - \sqrt{3}M}{2} = 1 - \frac{\sqrt{3}M}{2} \quad (2.26)$$

The boost factor B and the voltage gain G can be calculated as follows

$$B = \frac{1}{1 - 2\frac{T_o}{T}} = \frac{1}{\sqrt{3}M - 1} \quad (2.27)$$

$$G = \frac{\hat{v}_o}{V_{dc}/2} = MB = \frac{M}{\sqrt{3M-1}} \quad (2.28)$$

The curve of voltage gain versus modulation index is shown in Fig. 2.15. The voltage gain approaches infinity when M decreases to $\frac{\sqrt{3}}{3}$

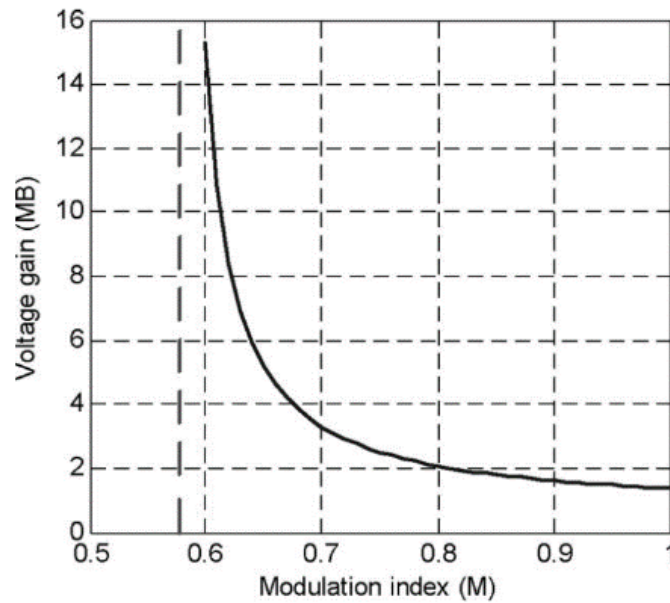


Figure 2.11 Voltage gain (MB) versus M

From Fig2.12, we can see that the upper shoot-through envelope is always equal to or higher than the maximum value of the reference signals, and the lower shoot-through envelope is always equal to or lower than the minimum value of the reference signals. Therefore, the shoot-through states only occur during the traditional zero states from the traditional carrier based PWM control. As a result, this control maintains the output waveform. It can be easily seen from the above analysis that the shoot-through duty ratio is always constant. This can be reconfirmed from a different perspective below. For modulation index M, the maximum active-state duty ratio $D_{a \max}$ can be expressed as

$$D_{a \max} = \max \left(\frac{M \sin \omega t - M \sin \left(\omega t - \frac{2\pi}{3} \right)}{2} \right) = \frac{\sqrt{3}}{2} M \quad (2.29)$$

Where $D_{a \max}$ is the maximum duty ratio of the active states combined in a switching cycle. In order to keep the active states unchanged while making the shoot-through duty ratio always constant, the maximum shoot-through duty ratio that can be achieved is

$$D_{o \max} = 1 - D_{a \max} = 1 - \frac{\sqrt{3}}{2} M \quad (2.30)$$

This is exactly the same as the results shown in (2.26). To summarize, this control method produces the maximum constant boost while minimizing the voltage stress.

The above-proposed maximum constant boost control (Fig. 2.12) can be implemented alternatively by using third harmonic injection. A sketch map of the third-harmonic injection control method is shown in Fig. 2.13. A third-harmonic component with 1/6 of the fundamental component is injected to the three phase-voltage references. As

shown in Fig. 2.13, V_a reaches its peak value $\frac{\sqrt{3}}{2} M$ while V_b is at its minimum value

$-\frac{\sqrt{3}}{2} M$ at $\frac{\pi}{3}$. Therefore, a unique feature can be obtained: only two straight lines,

V_p and V_n , are needed to control the shoot-through time with the $\frac{1}{6}$ (16%) third harmonic injection.

From Fig. 2.13, the shoot-through duty ratio can be calculated (2.26)

$$\frac{T_o}{T} = \frac{2 - \sqrt{3}M}{2} = 1 - \frac{\sqrt{3}M}{2} \quad (2.26)$$

which is identical to the previously proposed maximum constant boost-control method shown in Fig. 2.12. Therefore, the voltage gain can also be calculated by the same equations (2.27) and (2.28). The difference is that the third-harmonic-injection control

method has a larger modulation index M , which increased from 1 to $\frac{2\sqrt{3}}{3}$. The voltage gain versus M is shown in Fig. 2.8 for the third-harmonic-injection method. The

voltage gain can be varied from infinity to zero smoothly by increasing M from $\frac{\sqrt{3}}{3}$

to $\frac{2\sqrt{3}}{3}$ with shoot through, as shown in the

solid curve, and then decreasing M from $\frac{2\sqrt{3}}{3}$ to zero without shoot through, as shown

in the small dashed curve in Fig. 2.16 (Shen, et al., 2004)

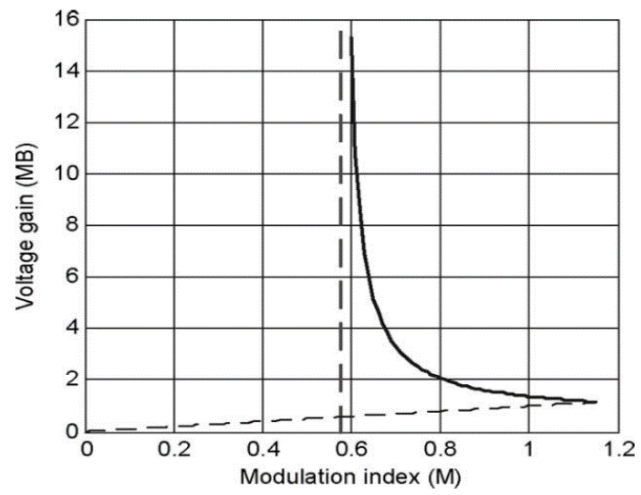


Figure 2.12 Voltage gain (MB) verses M in third harmonic injection

Chapter 3

Quasi-Z-Source Inverter

Chapter 3 Quasi-Z-Source Inverter

3.1 Introduction

The voltage fed ZSI has some significant drawbacks; namely that the input current is discontinuous in the boost mode and that the capacitors must sustain a high voltage. The main drawback of the current fed ZSI is that the inductors must sustain high currents. Also, control complexity is an issue when the ZSI is used in a back-to-back configuration due to the coupling of the inverter switching functions. To improve on the traditional ZSIs, four new quasi-Z-source inverters, qZSIs, have been developed which feature several improvements and no disadvantages when compared to the traditional ZSIs. The voltage fed ZSI as well as the two novel voltage fed inverters, with similar properties to the ZSI, are shown in Figs. 2.2, 3.1, and 3.2. The novel qZSI topologies shown in Figs. 3.1 and 3.2. The qZSI, shown in Fig. 3.1, when compared to the ZSI shown in Fig.2.2, features lower DC voltage on capacitor C2 as well as continuous input current, while the qZSI topology, shown in Fig. 3.2, features lower DC voltage on capacitors C1 and C2, however, the input current is discontinuous. Also, due to the input inductor, L1, the qZSI shown in Fig. 3.1 does not require input capacitance, unlike the ZSI and the qZSI shown in figure 3.2 . (Anderson & Peng, 2008)

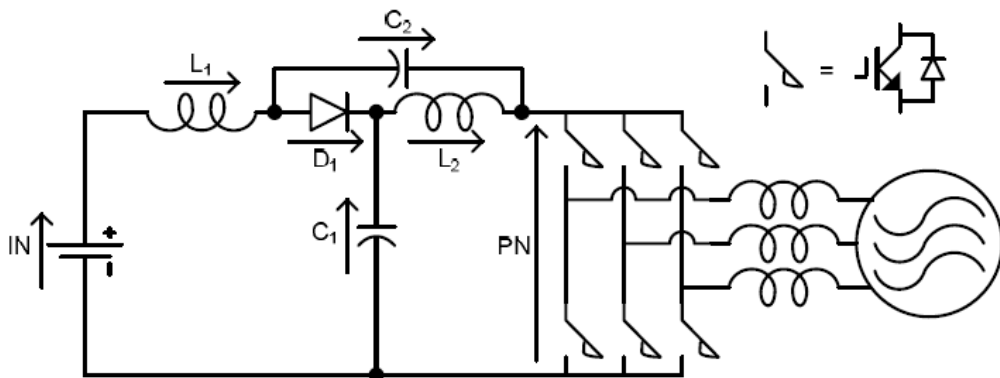


Figure 3.1 Voltage Fed qZSI with Continuous Input Current

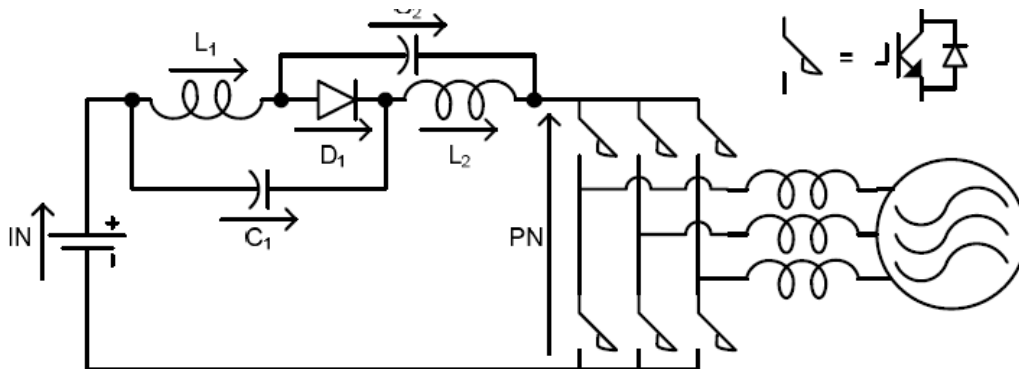


Figure 3.2 Voltage Fed qZSI with Discontinuous Input Current

By using the new quasi-Z-source topology in Fig 3.1, the inverter draws a constant current from the PV array and is capable of handling a wide input voltage range. It also features lower component ratings and reduced source stress compared to the traditional ZSI.

The traditional ZSI, and the qZSI has two types of operational states at the DC side: the nonshoot-through states (i.e. the six active states and two conventional zero states of the traditional VSI) and the shoot-through state (i.e. both switches in at least one phase conduct simultaneously).

In the non-shoot-through states, the inverter bridge viewed from the DC side is equivalent to a current source. The equivalent circuits of the two states are as shown in Figs. 3.3 and 3.4 the shoot-through state is forbidden in the traditional VSI, because it will cause a short circuit of the voltage source and damage the devices. With the qZSI and ZSI, the unique LC and diode network connected to the inverter bridge modify the operation of the circuit, allowing the shoot-through state. This network will effectively protect the circuit from damage when the shoot-through occurs and by using the shoot-through state, the (quasi-) Z-source network boosts the DC-link voltage. The major differences between the ZSI and qZSI are:

The qZSI draws a continuous constant DC current from the source while the ZSI draws a discontinuous current.

The voltage on capacitor C2 is greatly reduced. The continuous and constant DC current drawn from the source with this qZSI make this system especially well-suited for PV power conditioning systems.

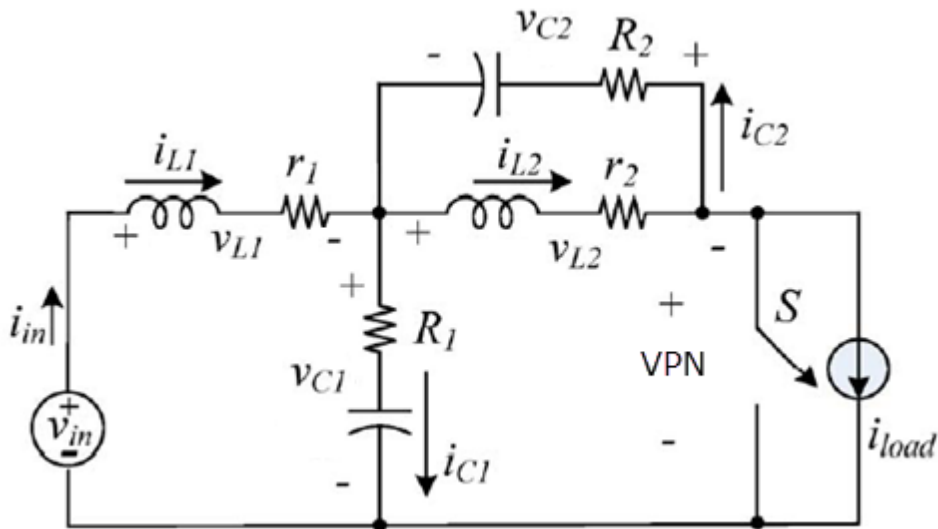


Figure 3.3 Equivalent circuit of the qZSI in non-shoot-through states

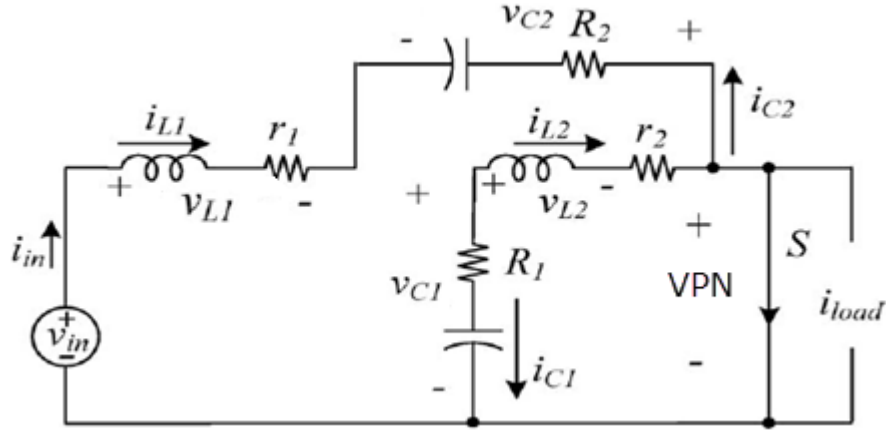


Figure 3.4 Equivalent circuit of the qZSI in shoot-through states

Regards to the two fig 3.3&3.4 with Assuming that during one switching cycle, T , the interval of the shoot through state is T_o ; the interval of non-shoot-through states is T_1 ; thus one has $T = T_o + T_1$ and the shoot through duty ratio, $D_o = T_o / T$. From Fig 3.3 which is a representation of the inverter during the interval of the non-shoot-through states, T_1 , one can get

$$V_{L1} = V_{in} - V_{C1}, \quad V_{L2} = -V_{C2} \quad (3.1)$$

$$V_{PN} = V_{C1} - V_{L2} = V_{C1} + V_{C2} \quad V_{diode} = 0. \quad (3.2)$$

From Fig 3.4 which is a representation of the system during the interval of the shoot-through states, T_o , one can get

$$V_{L1} = V_{C2} + V_{in}, \quad V_{L2} = V_{C1}, \quad (3.3)$$

$$V_{PN} = 0 \quad V_{diode} = V_{C1} + V_{C2}. \quad (3.4)$$

At steady state, the average voltage of the inductors over one switching cycle is zero. From (3.1), (3.2), one has

$$V_{L1} = \overline{v_{L1}} = \frac{T_o(V_{C2} + V_{in}) + T_1(V_{in} - V_{C1})}{T} = 0$$

$$V_{L2} = \overline{v_{L2}} = \frac{T_o(V_{C1}) + T_1(-V_{C2})}{T} = 0$$

Thus

$$V_{C1} = \frac{T_1}{T_1 - T_o} V_{in} \quad V_{C2} = \frac{T_o}{T_1 - T_o} V_{in} \quad (3.5)$$

From (3.2), (3.4) and (3.5), the peak DC-link voltage across the inverter bridge is

$$\overline{v_{PN}} = V_{C1} + V_{C2} = \frac{T_o}{T_1 - T_o} V_{in} = \frac{1}{1 - 2\frac{T_o}{T}} V_{in} = B V_{in} \quad (3.6)$$

Where B is the boost factor of the qZSI. This is also the peak voltage across the diode. The average current of the inductors L₁, L₂ can be calculated by the system power rating P

$$I_{L1} = I_{L2} = I_{in} = P / V_{in} \quad (3.7)$$

According to Kirchoff's current law and (3.7), we also can get that

$$I_{C1} = I_{C2} = I_{PN} - I_{L1} \quad I_D = 2I_{L1} - I_{PN} \quad (3.8)$$

In summary, the voltage and current stress of the qZSI are shown in Table 1. The stress on the ZSI is shown as well for comparison, where M is the modulation index; $\overline{v_{in}}$ is the AC peak phase voltage; P is the system power rating;

$$m = \frac{T_1}{T_1 - T_o} \quad ; n = \frac{T_o}{T_1 - T_o} \quad ; \text{thus } m > 1 \quad ; m - n = 1;$$

$$B = \frac{T_1}{T_1 - T_o}, \text{ thus } m + n = B, 1 < m < B.$$

From Table 3.1 we can find that the qZSI inherits all the advantages of the ZSI. It can buck or boost a voltage with a given boost factor. It is able to handle a shoot through state, and therefore it is more reliable than the traditional VSI. It is unnecessary to add a dead band into control schemes, which reduces the output distortion. In addition, there are some unique merits of the qZSI when compared to the ZSI:

The two capacitors in ZSI sustain the same high voltage; while the voltage on capacitor C2 in qZSI is lower, which requires lower capacitor rating;

The ZSI has discontinuous input current in the boost mode; while the input current of the qZSI is continuous due to the input inductor L₁, which will significantly reduce input stress; For the qZSI, there is a common DC rail between the source and inverter, which is easier to assemble and causes less EMI problems

Table 3.1 Voltage and average current of the qZSI and ZSI network

	vL1=vL2		vPN		vdiode	
	T0	T1	T0	T1	T0	T1
ZSI	mV _{in}	-nV _{in}	0	BV _{in}	BV _{in}	0
qZSI	mV _{in}	-nV _{in}	0	BV _{in}	BV _{in}	0
	VC1		VC2		$\overline{v_{in}}$	
ZSI	mV _{in}		mV _{in}		MBV _{in} / 2	
qZSI	mV _{in}		mV _{in}		MBV _{in} / 2	
	I _{in} = I _{L1} = I _{L2}		I _{C1} = I _{C2}		I _D	
ZSI	P / V _{in}		I _{PN} - I _{L1}		2I _{L1} - I _{PN}	
qZSI	P / V _{in}		I _{PN} - I _{L1}		2I _{L1} - I _{PN}	

If the inverter is operated entirely in the non-shoot-through states (Fig. 3.3) the diode will conduct and the voltage on capacitor C1 will be equal to the input voltage while the voltage on capacitor C2 will be zero. Therefore, in $v_{PN}=V_{in}$ and the qZSI acts as a traditional VSI:

$$\bar{v}_{ln} = \frac{\bar{V}_{PN}}{2} \bullet M = \frac{V_{in}}{2} \bullet M \quad (3.9)$$

For SPWM $0 \leq M \leq 1$. Thus when $D = 0$, \bar{v}_{ln} is always less than $V_{in}/2$ and this is called the buck conversion mode of the qZSI. By keeping the six active states unchanged and replacing part or all of the two conventional zero states with shoot-through states, one can boost V_{PN} by a factor of B , the value of which is related to the shoot-through duty ratio, as shown in (3.7). This is called the boost conversion mode of the qZSI. (Li, Anderson, Peng, & Liu, 2009)

$$\text{The peak AC voltage becomes } \bar{v}_{ln} = \frac{\bar{V}_{PN}}{2} \bullet M = \frac{V_{in}}{2} \bullet B \bullet M \quad (3.10)$$

3.2 Quasi-Z-Source Inverter Design

The inverter which will be designed here is 10KW rated power with 60Hz 208 V VL-L (rms). (Li, Anderson, Peng, & Liu, 2009)

This inverter is supplied by DC Voltage source (200-400)VDC, the inverter parameters are described in table 3.2

Table 3.2 The main parameters of inverter

Rated Power	10KW
DC input	200-400 VDC
Output AC Voltage	208V VL-L (rms)
Frequency	60Hz
Carrier Frequency	10 kHz

The maximum voltage gain G will be with 200v DC:

$$G_{\max} = \frac{\hat{V}_{AC}}{V_{dc}/2} = \frac{\frac{208}{\sqrt{3}} \bullet \sqrt{2}}{\frac{200}{2}} = 1.698$$

To get the maximum voltage gain we have to apply the minimum modulation index M which will be calculated by:

$$M_{\min} = \frac{G_{\max}}{\sqrt{3} \bullet G_{\max} - 1} = \frac{1.698}{\sqrt{3} \bullet 1.698 - 1} = .875$$

With the same maximum voltage gain G and minimum modulation index M we get the maximum boost factor B can be calculated by:

$$B_{\max} = \frac{1}{\sqrt{3} * M_{\min} - 1} = \frac{1}{\sqrt{3} * .875 - 1} = 1.939$$

The maximum voltage stress on the inverter bridge can be calculated by:

$$V_{\text{stress}} = B_{\max} * V_{dc} = 1.939 * 200 = 387.8$$

The maximum current in inductor can be calculated by:

$$I_{in} = I_{L1} = I_{L2} = \frac{P}{V_{dc}} = \frac{10000}{200} = 50A$$

The frequency of carrier is 10 KHz so the shoot-through frequency is doubled to 20 kHz so the maximum T_o can be calculated by:

$$T_{o_max} = 2 * \frac{1 - \frac{\sqrt{3} * M_{\min}}{2}}{20000} = 0.0000242 \text{sec}$$

The inductors in the qZSI network limit the ripples of current during boost conversion mode, choosing the acceptable peak to peak current ripple $rc\%$ to be 20% can be calculated by:

$$rc\% = .2 * 50 = 10$$

$$m = \frac{T1}{T1 - T_o} = \frac{.0000758}{.0000758 - .0000242} = 1.468$$

$$n = \frac{T_o}{T1 - T_o} = \frac{.0000242}{.0000758 - .0000242} = .468$$

$$L = \frac{m * V_{dc} * T_{o \max}}{rc\% * 2} = .000355 = 355 \mu H$$

These two capacitors absorb the current ripple and limit the voltage ripple on the inverter bridge and to keep the output voltage sinusoidal. Choosing the acceptable voltage ripple $rv\%$ to be 1% can be calculated by:

$$rv\% = .01 * 200 = 2$$

$$C = 2 * \frac{I_{in} * T_{o \max}}{B * rv\% * 2} = .0000311 = 311 \mu F$$

A model of the qZSI as fig 3.3&3.4 was tested with these parameters in table 3.3:

Table 3.3 The parameters of qZSI network

Parameter	Value
L	500 μ H
C	400 μ F
r	0.235 Ω
R	0.07 Ω
Lf	1000 μ H
Cf	100 μ F
Rload	10 Ω

Chapter 4

Quasi-Z-Source Inverter Controller Design

Chapter 4 Quasi-Z-Source Inverter Controller Design

4.1 Calculations of M and Do

The controller in this thesis will work in two different methods, the first method is boosting the DC input voltage less than $\sqrt{2} * 208 = 294$ and the second method will be bucking when the input voltage above $\sqrt{2} * 208 = 294$.

The method used in this controller was mamdani with 115 rules as described in appendix A.

According to these relationships for Boost:

$$G = \frac{\hat{V}_{AC}}{V_{dc}/2}$$

$$M = \frac{G}{\sqrt{3} * G - 1}$$

$$D_o = 1 - \frac{\sqrt{3} * M}{2}$$

$$m = \frac{T_1}{T_1 - T_o}$$

$$n = \frac{T_o}{T_1 - T_o}$$

$$V_{c1} = mV_{dc}$$

$$V_{c2} = nV_{dc}$$

$$B = \frac{1}{\sqrt{3} * M - 1}$$

$$V_{stress} = B * V_{dc}$$

According to these relationships for Buck:

$$G = M = \frac{2 * 208 * \sqrt{2}}{V_{dc} * \sqrt{3}}$$

$$D_o = 0$$

$$V_{c1} = V_{dc}$$

$$V_{c2} = 0$$

And choosing samples of VDC ; values below than $\sqrt{2} * 208 = 294$ the inverter must work in boost and values which above 294 must work in buck with these values in table 4.1:

Table 4.1 Samples of VDC

VDC	M	Do	Mode
200	0.875	0.242	Boost
220	0.922	0.201	Boost
240	0.953	0.174	Boost
260	1.016	0.120	Boost
280	1.102	0.046	Boost
292	1.146	0.007	Boost
294	1.150	0	Buck
296	1.148	0	Buck
312	1.089	0	Buck
332	1.023	0	Buck
352	0.965	0	Buck
372	0.913	0	Buck
392	0.866	0	Buck

For boosting seven samples of vDC from 200 to 292 v and the values of modulation Index M and Duty ratio Do was calculated.

For Bucking the only values must calculated is only modulation index M and fixed zero value for duty ratio Do; another seven samples was chosen from 294 to 392.

4.2 Fuzzy Controller Memberships

4.2.1 Introduction

In this thesis the controller have three inputs and two outputs, the three inputs was chosen as below:

VDC: This input take care of the statues of source voltage, so that the controller must take the decision for work as boost or buck and the values of M and Do.

IDC: This input take care of the statues of current in inductor in quasi-Z-source network, so the controller give the value of Do to limit the current as possible.

Vc1: The value of Vc1 give the reached value of boosting voltage, so the controller give values of M and Do to keep it 294 if input VDC is below the 294, and if its above this input is not considered.

The two outputs of controller are used in this thesis separately to control the output voltage and current in inductor, these two outputs are:

M: modulation index M can be $\frac{\sqrt{3}}{3}$ to $\frac{2\sqrt{3}}{3}$ in boosting; the less M in boosting give the max boost and an be from 0 to 1 in bucking; the maximum M in buck give the minimum buck. (Shen, et al., 2004)

Do: duty ratio Do have a job just in boosting and can control the current in inductor but must keep the relation $M \leq \frac{2}{\sqrt{3}}(1 - Do)$ to avoid distortion of output signal. (Li, Jiang, Cintron-Rivera, & Peng, 2013)

4.2.2 VDC Input

Memberships (200,220,240,260,280,292) was chosen for boost because of values in of input voltage in this region is below 294,and memberships (294, 296,312,332,352,372,392) was chosen for buck because of values in of input voltage in this region is above 294 ,all the memberships are described in table 4.2

Table 4.2Memberships of VDC Input

Membership Name			
200	180	200	220
220	200	220	240
240	220	24	260
260	240	260	280
280	260	280	292
292	280	292	294
294	292	294	296
296	294	296	312
312	296	312	332
332	312	332	352
352	332	352	372
372	352	372	392
392	372	392	412

All the memberships are trimf, the narrowest membership is 294 because the centre of this membership is 294 the critical point in this input as described in fig 4.1.

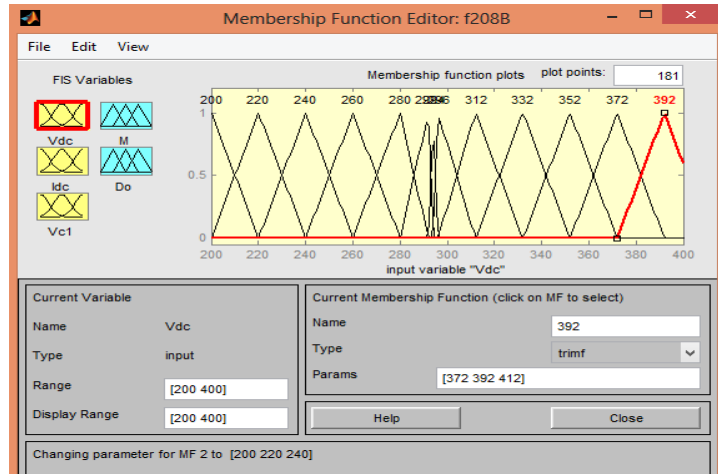


Figure 4.1 Memberships Functions of VDC Input

4.2.3 IDC Input

The aim of choosing this input is keeping the current in inductor the minimum as possible as I can to reduce the radius of inductor wire, the memberships as described in table 4.3.

Table 4.3 Memberships of IDC Input

Membership Name				
292(34.25)	-5	0	34.25	35.71
280(35.714)	34.25	35.71		38.46
260(38.462)	35.71	38.46		41.67
240(41.667)	38.46	41.67		45.45
220(45.455)	41.67	45.45		50
200(50)	45.45	50	80	85

The memberships (292(34.25) and 200(50)) are trampf because the lowest current value of 10kw load is at 292 volt with 34.5 amp and the highest current value of 10kw load is at 200 volt with 50 amp.

The other memberships are rtmf as fig 4.2.

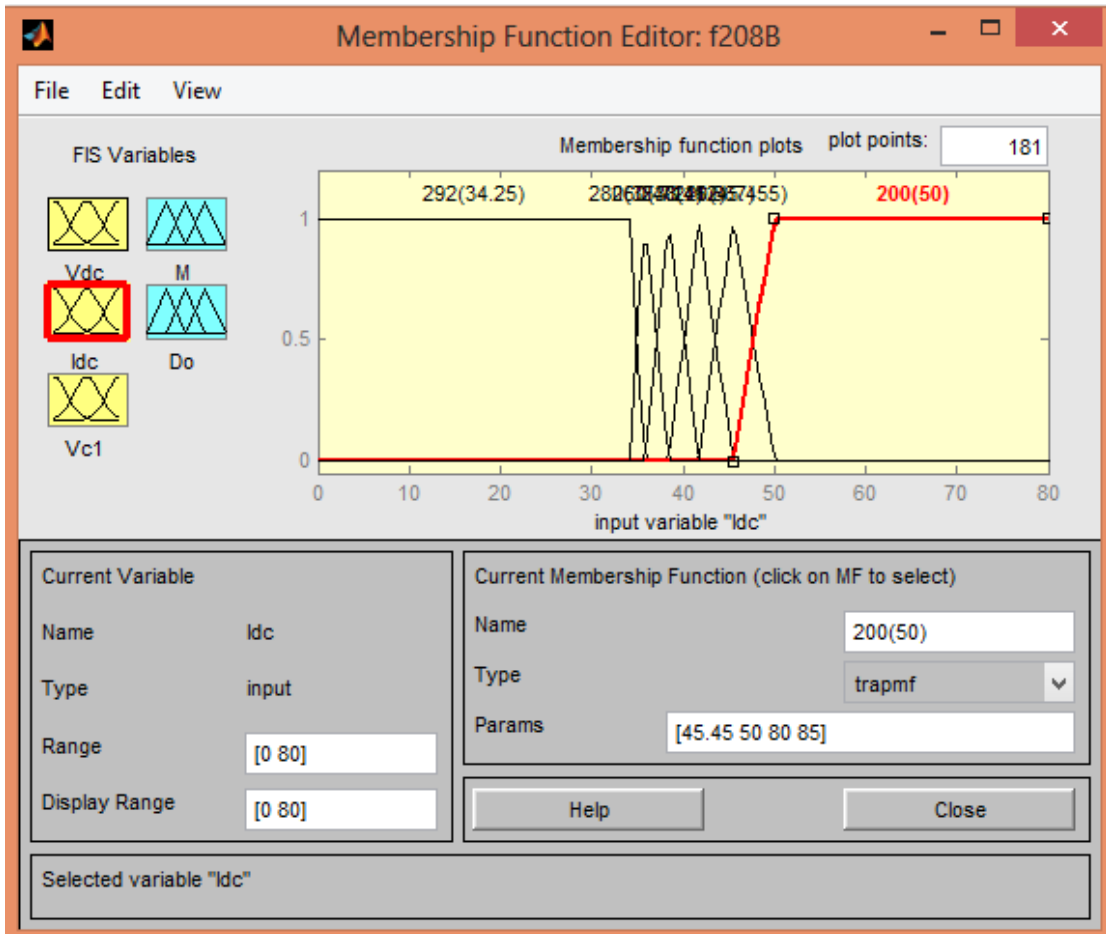


Figure 4.2 Memberships Functions of IDC Input

4.2.4 Vc1 Input

The aim of choosing this input is keeping the output voltage constant to 294 volt whatever the input voltage within the boost range of (200-294) ,the memberships are described in table 4.4.

Table 4.4Memberships of Vc1 Input

Membership Name				
290	96	100	290	294
294	290	294		298
298	294	298	396	400

The memberships (290 and 298) are trapezoidal because the input value of range of 290 membership make the controller work in boosting and the input value of range of 298 membership make the controller work in bucking.

The other membership 294 is rtmf because this is the critical membership as fig 4.3.

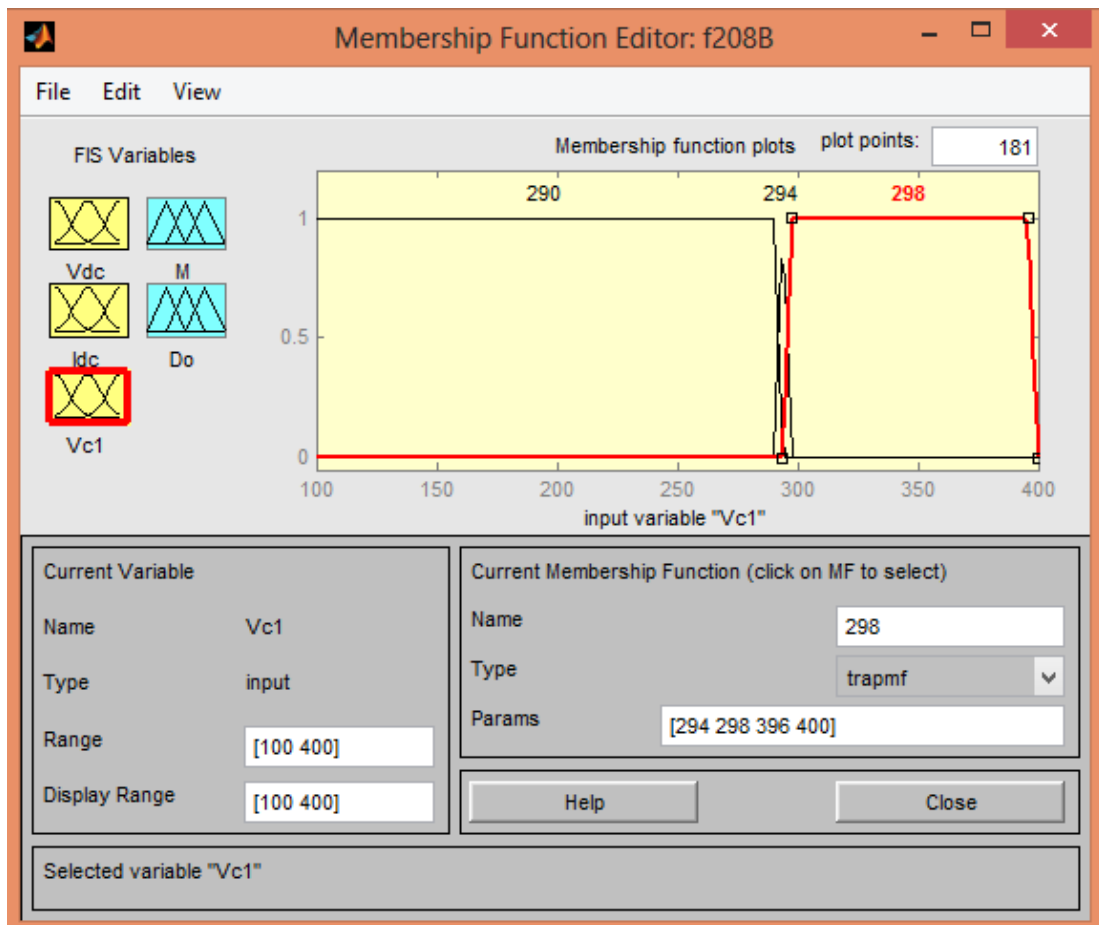


Figure 4.3 Memberships Functions of Vc1 Input

4.2.5 M output

The aim of choosing this input is keeping the output voltage constant to 294 volt whatever the input voltage within the boost range of (200-400).

The memberships (2,4,5,7,10) in table 4.5 are used in boosting and memberships (1,3,6,8,9,12) in table 4.5 are used in bucking .

Table 4.5 Memberships of M Output

#	Membership Name			
1	392(0.866)	0.857	0.866	0.875
2	200(0.875)	0.866	0.875	0.913
3	372(0.913)	0.875	0.913	0.922
4	220(0.922)	0.913	0.922	0.954
5	240(0.953)	0.922	0.954	0.965
6	352(0.965)	0.954	0.965	1.016

7	260(1.016)	0.965	1.016	1.023
8	332(1.023)	1.016	1.023	1.089
9	312(1.089)	1.023	1.089	1.102
10	280(1.102)	1.089	1.102	1.146
11	292(1.146)	1.102	1.146	1.148
12	296(1.148)	1.146	1.148	1.150
13	294(1.150)	1.148	1.150	1.152

All the memberships in table 4.5 are trimf, described in fig 4.4.

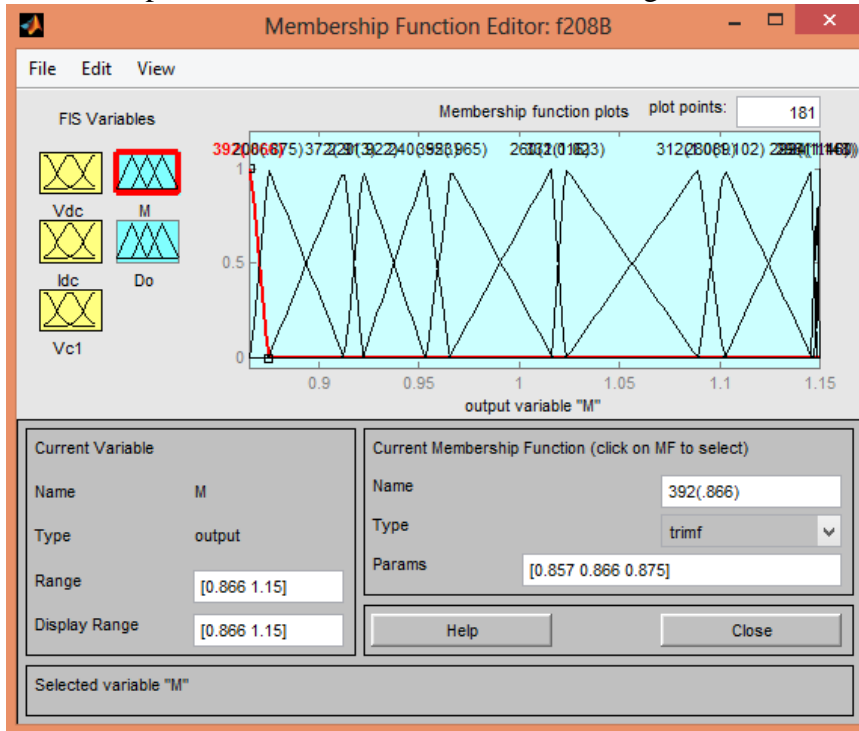


Figure 4.4 Memberships Functions of M Output

4.2.6 Do Output

The aim of choosing this output is keeping the current in inductor to the minimum as possible as I can to reduce the radius of inductor wire, the memberships as described in table 4.6.

Table 4.6 Memberships of Do Output

Membership Name			
0	-0.007	0	0.007
292(0.007)	0	0.007	0.046
280(0.046)	0.007	0.046	0.120
260(0.120)	0.046	0.120	0.174
240(0.174)	0.120	0.174	0.201
220(0.201)	0.174	0.201	0.242
200(0.242)	0.201	0.242	0.283

All the memberships in table 4.6 are trimf, described in fig 4.5.

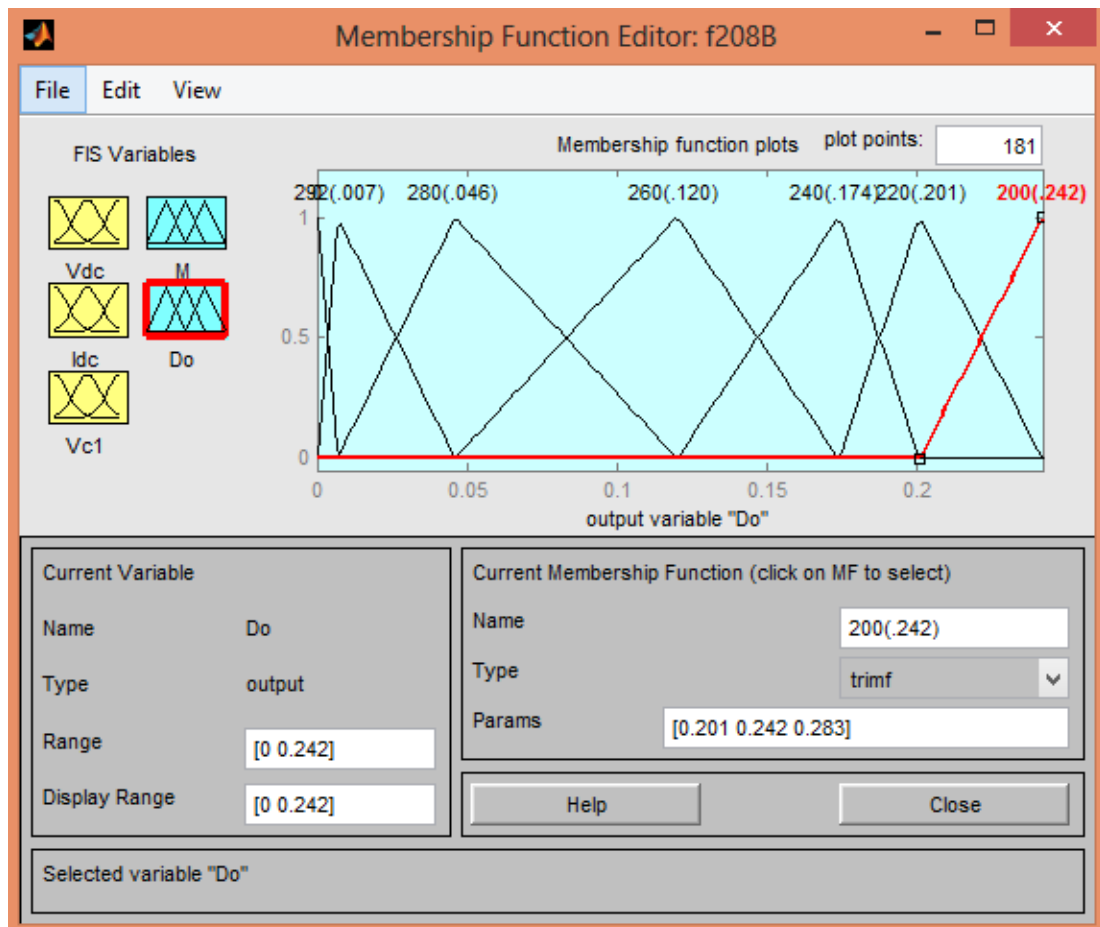


Figure 4.5 Memberships Functions of Do Output

4.3 Surfaces

M Output

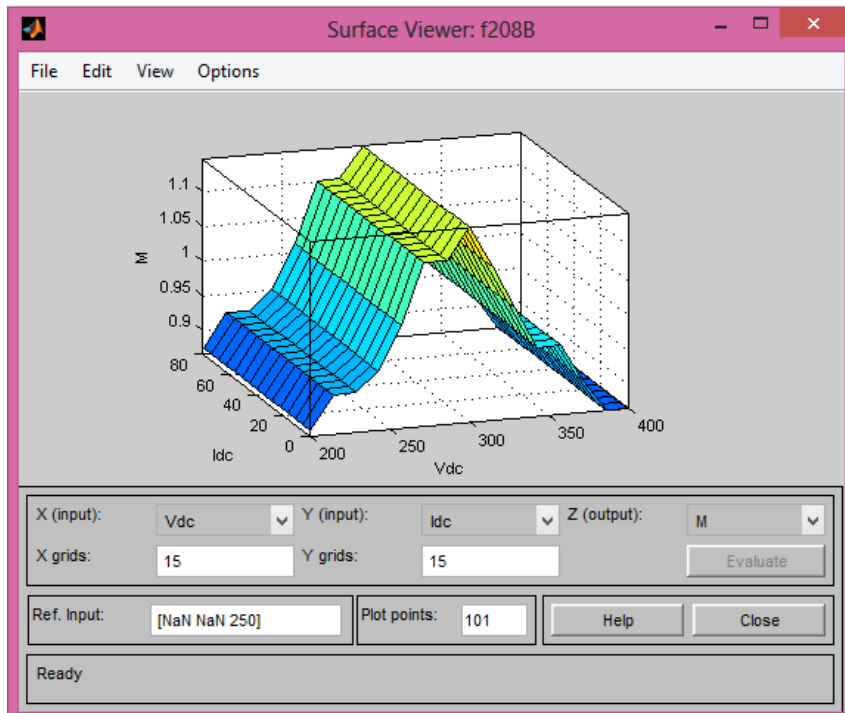


Figure 4.6 Surface for M Output

Do Output

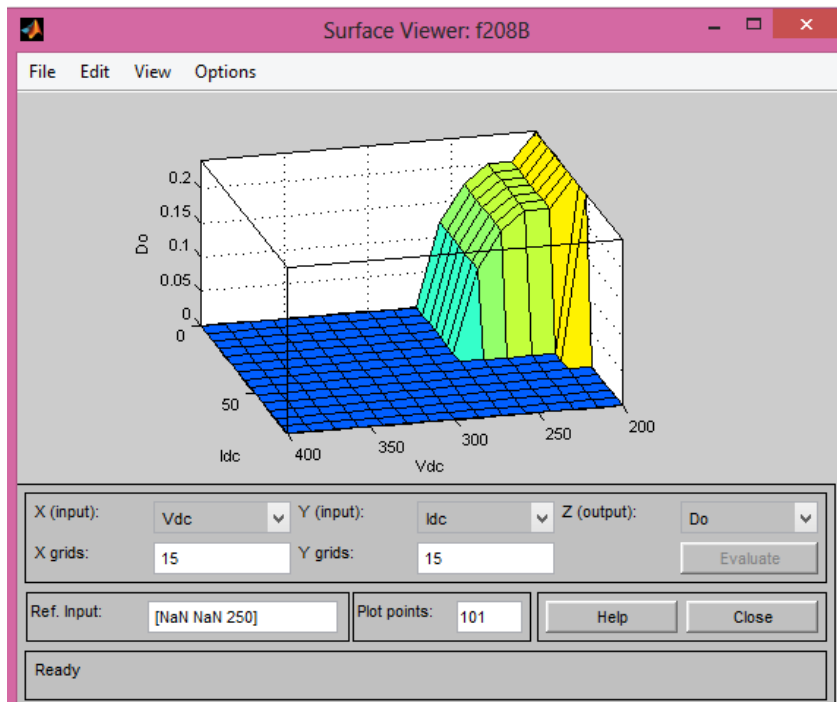


Figure 4.7 Surface for Do Output

4.4 Simulink Model

In this thesis Matlab Simulink used for simulation because of its wide element exist in Simulink libraries; the Simulink model as shown in fig 4.8 consist of:

Variable DC Block :is a sin wave source shifted 200 in x axis and peak to peak 200 also with 5 Hz frequency connected to (controlled voltage source) to give variable DC source [200-400].

Quasi Z Source: this block contain quasi-Z-Source network as in fig 3.1 with values of L,C,r,R and Rload as in table 3.3.

Universal Bridge: this is 3 bridge arms of IGBT to work as switches for three phase inverter switches.

Filter: This filter is LC filter with values of Lf and Cf as in table 3.3.

Fuzzy Logic Controller: This Fuzzy controller contain the fuzzy system described in section 4.2.

Scope: this Scope consist of 6 axis

- DC Input
- DC Input Current.
- Three-phase voltage waves.
- Three-phase current waves.
- Voltage stress cross switches.
- Output voltage line-line rms.

Pulses: This block is described in fig4.9 and contain.

Three sine wave with third harmonic injection reference signals, the phase shift between each other is 120 degree and the peak value changes as M change, the peak of third harmonic injected signal is $\frac{\sqrt{3}}{2}M$ as mentioned in page 21 ,so if the M=1.15 the peak of reference will be 1.

Triangular wave generator with 10KHz frequency as carrier signal and fixed peak value of 1.

Comparators to choose the system will operate in boosting or bucking.

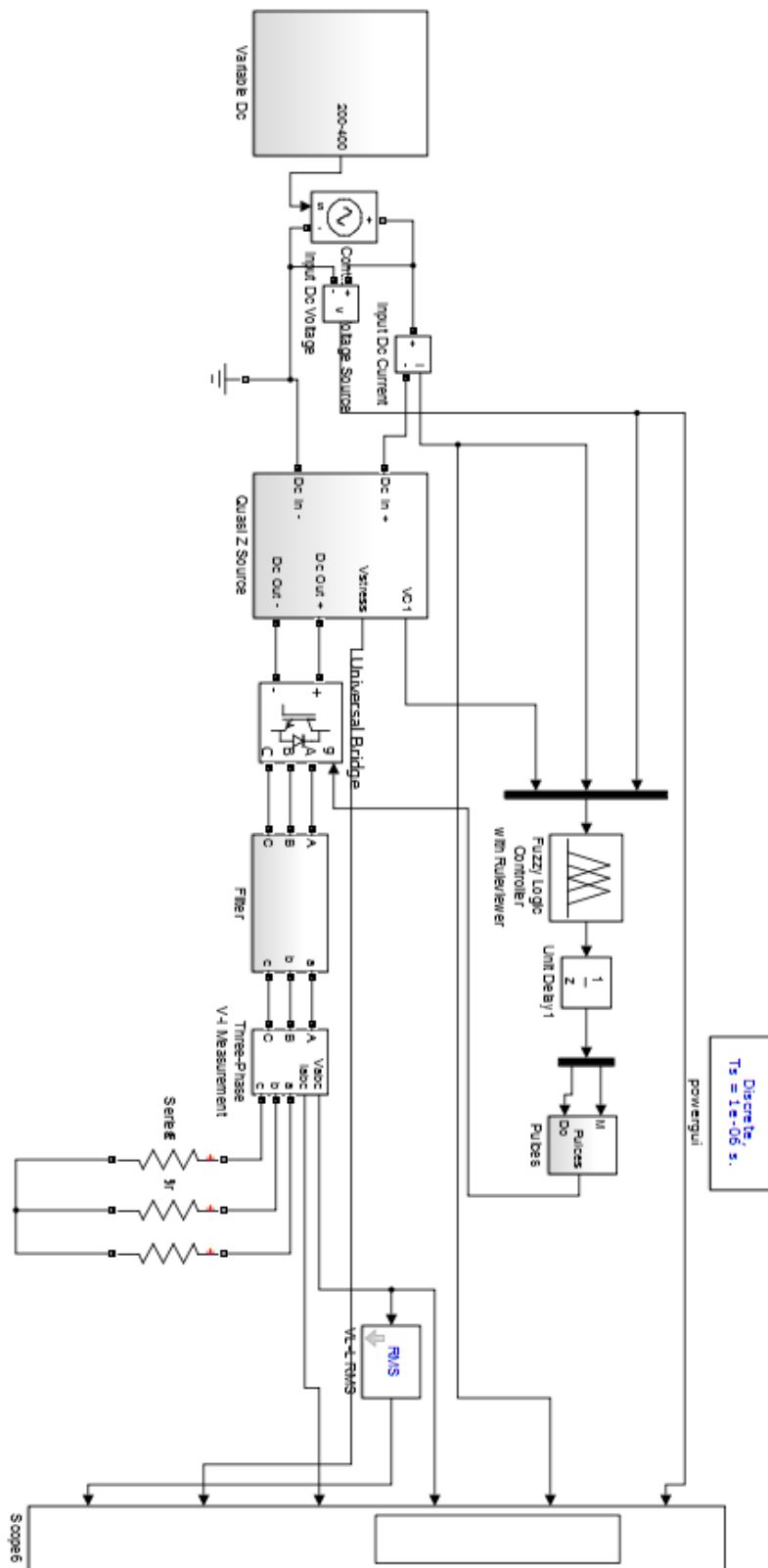


Figure 4.8 Simulink Model of all system

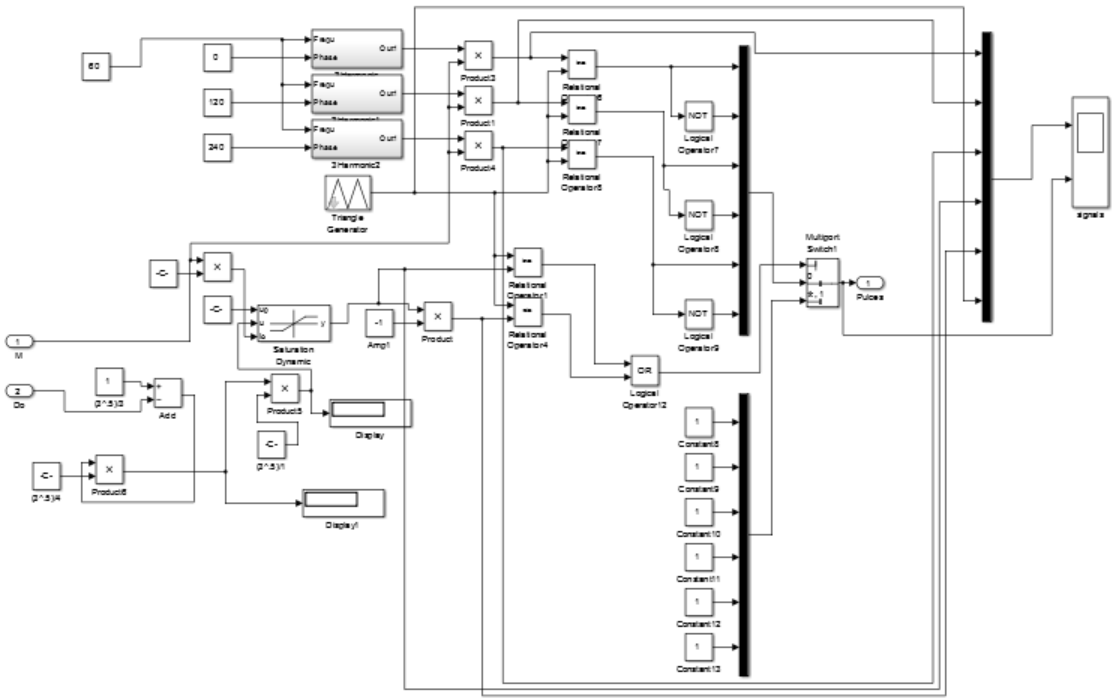


Figure 4.9 Pulses Block

4.5 Results

The simulation for the designed Fuzzy Controller described in section 4.2 in the system designed in table 3.3 with applying variable DC input (200-400)v is shown in fig 4.10 .It is clear that the output voltage rms is in range of (206-209)rms L-Line.

In fig 4.10 the system simulated for 0.2 second as one period of the DC source block, the voltage in 0 s is 200 v and in 0.1 sec is 400 and go back to 200 by 0.2sec.

Changing in DC input keep the rms value of output rms (206-209) volt with fixed load 10 KW.

Value of current is inversely proportional to input DC voltage except in the first of operating the energy absorbed from source is more than 10KW it about 15KW.

The output signal is pure sine wave in voltage and current.

The voltage stress is about 400 and the calculated in page 28 was 387 v

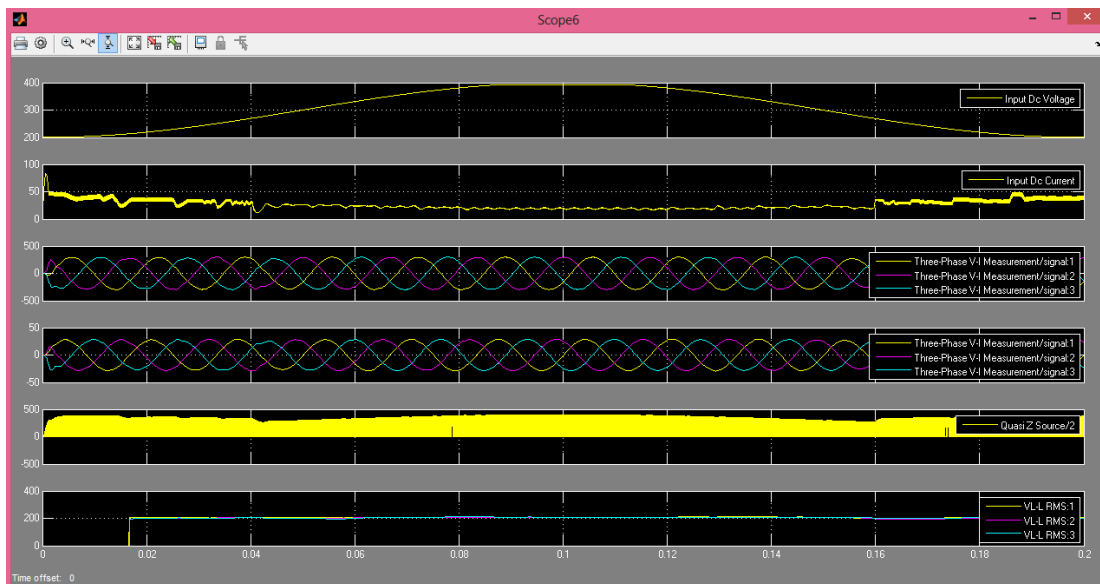


Figure 4.10 Results of Variable VDC Input (200-400)

I tried the same system with fixed input DC voltage to 200 v for 0.025 sec with fuzzy controller in fig 4.11 ,and no controller in fig 4.12 with fixed values of M and Do as calculated in page 28 and 31 $M= 0.875$ and $Do =0.242$.

The result of fuzzy controlled system was in fig 4.11 and the maximum DC current was 75 A which mean the system with load 10KW absorbs 15Kw for for a little while, but the no fuzzy controlled system the maximum DC current was 145 A absorbs 29Kw, these advantage accrued by controlling M and Do indecently.

The another point I noticed is voltage stress ,in non-controlled system with 200 v DC input the maximum voltage stress was 500 v but in fuzzy controlled one was 400v.

By the designed fuzzy controller the reduced current in inductor mean reducing the cross section in inductor wire and reducing weight and volume of device, and of course increasing the efficiency of inverter in solar systems.

Reducing voltage stress mean cheaper switches and less heat in device.

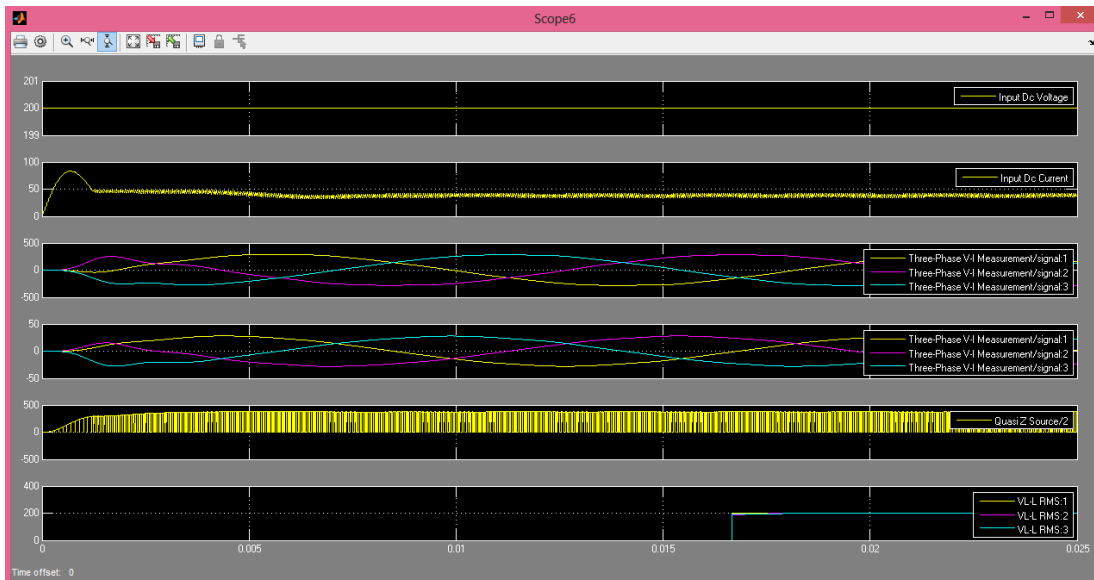


Figure 4.11 Result of Fixed Input 200 V DC with fuzzy controller.

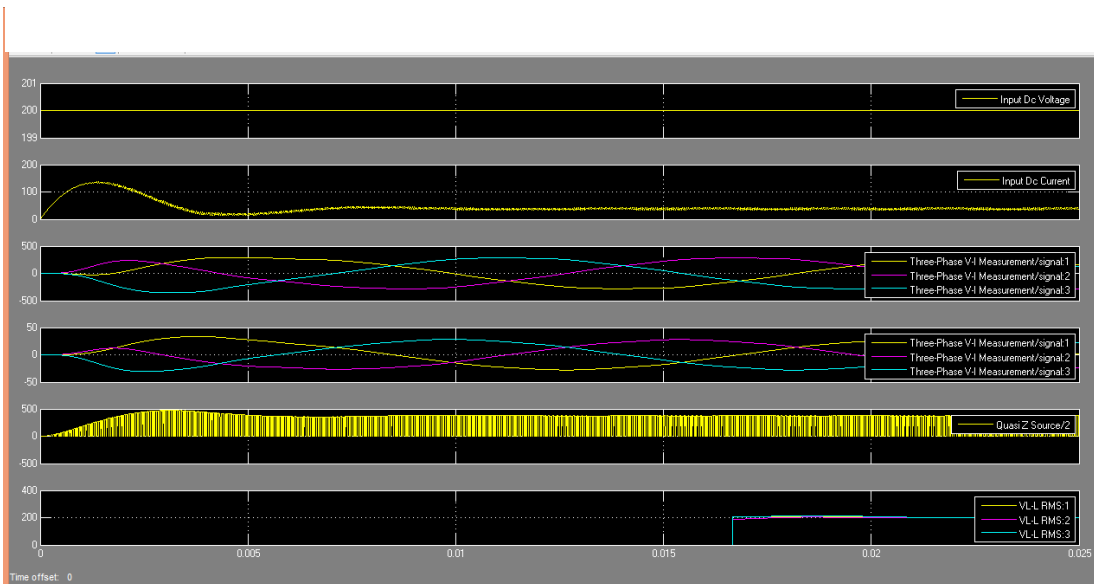


Figure 4.12 Result of Fixed Input 200 V DC without controller

Chapter 5

Conclusion and Future Research

Chapter 5 Conclusion and Future Research

5.1 Conclusions

Nowadays electrical energy converting plays an important role in industries and daily life, especially DC-AC inverters, because of existing many DC sources like batteries, solar panels and super capacitors; besides to motor inverters applications.

Z-source inverter discussed briefly in this thesis with its ability to work buck & boost and overcome regular inverter limitations.

To overcome Z-Source inverter disadvantages quasi-Z-source inverter described and analysed.

Related on previous background 10KW quasi-Z-Source designed and controlled by fuzzy controller.

In this research I applied Fuzzy controller with three inputs (VDC, IDC and Vc1) and two outputs (M and Do), this fuzzy controller contain 115 rule with mamdani method. Fuzzy controller controlled the main input parameters of quasi-z-source M&Do separately, with this technique I could control the input current DC and the output voltage AC separately, in the simulation result it clear that the output voltage was constant to 208 VL-L rms with wide range of input DC voltage (200-400)v, and I could minimize the current in inductor to half which minimize the size and weight of device.

5.2 Future Work

In this thesis mamdani method was used in fuzzy controller, it will be very important and helpful to compare it with sugeno method.

The load here in this thesis was resistive load, it can be changed to variable power factor load and improve controller and filter design to achieve the perfect results.

References

- Anderson, J., & Peng, F. Z. (2008, June). Four Quasi-Z-Source Inverters. *IEEE PES*, 2743-2749.
- Dharmadhikari, P. S. (2013). Comparison of Full Bridge Voltage Source Inverter with Different PWM Techniques. *National Conference on Innovative Paradigms in Engineering & Technology*, 25-30.
- Ge, B., Abu-Rub, H., Peng, F. Z., Lei, Q., Almeida, A. T., Ferreira, F. J., . . . Liu, Y. (2013, October). An Energy-Stored Quasi-Z-Source Inverter for Application to Photovoltaic Power System. *IEEE Transactions on Industrial Electronics*, 60(10), 4468-4481.
- Husodo, B. Y., Ayoub, S. M., Anwari, M., & Taufik. (2013, May). Simulation of Modified Simple Boost Control for Z-Source Inverter. *International Journal of Automation and Power Engineering*, 2(4), 57-64.
- Laxmi, G. J., & Ro, J. R. (2013, November). Multi Switching Techniques of Z-Source Inverter based PMSM Drive. *International Journal of Engineering Research & Technology*, 2(11), 4215-4223.
- Li, X., Yan, Z., Pan, K., Ma, C., & Qi, H. (2013). The Control Technology Research of the Z-Source Three Phase Four Bridge Arm Inverter. *Energy and Power Engineering*, 733-739.
- Li, Y., Anderson, J., Peng, F. Z., & Liu, D. (2009). Quasi-Z-Source Inverter for Photovoltaic Power Generation Systems. *24th IEEE APEC*, 918-924.
- Li, Y., Jiang, S., Cintron-Rivera, J. G., & Peng, F. Z. (2013, April). Modeling and Control of Quasi-Z-Source Inverter for Distributed Generation Applications. *IEEE Transactions on Industrial Electronics*, 60(4), 1532-1541.
- Liu, Y., Gel, B., & Abu-Rub, H. (2013). Modelling and Controller Design of Quasi-Z-Source Cascaded Multilevel Inverter-Based Three Phase Grid Tie Photovoltaic Power System. *Renewable Power Generation*, 8(8), 925-936.
- Neeraj, M. K., Kumar, C. L., & J, S. H. (2015). Three Phase Voltage Source Inverter for Front End Rectifier Fed to AC-Motor Drive Using Matlab. *International Journal of Engineering Science and Innovative Technology*, 4(3), 221-226.
- Penchalababu, V., Chandarakala, B., & Karismna, G. (2012, June). A survey on Modified Simple Boost Control for Z-Source Inverter. *International Journal of Engineering and Advanced Technology*, 1(5), 556-562.
- Peng, F. Z. (MARCH/APRIL 2003). Z-Source Inverter. *IEEE TRANSACTIONS ON INDUSTRY APPLICATIONS*, VOL. 39, NO. 2, 39(2), 504-510.
- Ride, O., & Olszewski, M. (2005). Shoot-Through PWM Control. In *Z-Source Inverter for Fuel Vehicles* (pp. 39-45).

- Sathya, S., & Karthikeyan, C. (2013, July). Fuzzy Logic Based Z-Source Inverter for Hybrid Energy Resources. *International Journal of Engineering Science and Innovative Technology*, 2(4), 57-63.
- Shen, A. W., Pham, C.-T., Dzung, P. Q., Anh, N. B., & Viet, L. H. (2012, August). Using Fuzzy Logic Self-Tuning PI Gain Controller Z-Source Inverter in Hubrid Electric Vechicles. *Irternational Journal of Engineering and Technolgy*, 4(4), 382-387.
- Shen, M., Wang, J., Joseph, A., Peng, F. Z., Tolbert, L. M., & Adams, D. J. (2004). Maximum Constant Boost Control of the Z-Source Inverter. *IAS IEEE*, 142-147.
- Shen, M., Wang, J., Peng, F. Z., Tolbert, L. M., & Adams, D. J. (2006, May/June). Constant Boost Control of the Z-Source Inverter to Minimize Current Ripple and Voltage Stress. *IEEE Transaction on Industry Applications*, 42(3), 770-778.
- Shete, P. S., Kanojiya, R. G., & Maurya, N. S. (2012). Performance of Sinusoidal Pulse Width Modulation based Three Phase Inverter. *International Confrance on Emerging Frotiers in Technology for Rural Area*, 22-26.
- Siwakoti, Y. P., Peng, F. Z., Blaabjerg, F., Loh, P. C., & Town, G. E. (2015, February). Impedance-Source Networks for Electric Power Conversion Part I:Review of Control and Modulation Techniques. *IEEE Transaction on Power Electronics*, 30(2), 699-716.
- Siwakoti, Y. P., Peng, F. Z., Blaabjerg, F., Loh, P. C., Town, G. E., & Yang, S. (2015, April). Impedance-Source Networks for Electric Power Conversion Part II:Review of Control and Modulation Techniques. *IEEE Transactions on Power Electronics*, 30(4), 1887-1906.
- Suresh, L., Kumar, G. N., & Sudarsan, M. V. (2012). *Modulation and Simulation of Z-Source Inverter*. Vadlamudi: Selected Works of suresh l.
- Vijayabalan, R., & Ravivarman, S. (2012, December). Z-Source Inverter for Photovoltaic System with Fuzzy Logic Controller. *International Journal of Power Electronics and Drive System*, 2(4), 371-379.

Appendices

Appendix A

Table Appendix. 1 Fuzzy Rules

	VDC	IDC	Vc1	M	Do
1	200	292(34.25)	290	200(0.875)	200(0.242)
2	200	292(34.25)	294	200(0.875)	200(0.242)
3	200	292(34.25)	298	220(0.922)	200(0.242)
4	200	280(35.714)	290	200(0.875)	200(0.242)
5	200	280(35.714)	294	200(0.875)	200(0.242)
6	200	280(35.714)	298	220(0.922)	200(0.242)
7	200	260(38.462)	290	200(0.875)	200(0.242)
8	200	260(38.462)	294	200(0.875)	200(0.242)
9	200	260(38.462)	298	220(0.922)	200(0.242)
10	200	240(41.667)	290	200(0.875)	200(0.242)
11	200	240(41.667)	294	200(0.875)	200(0.242)
12	200	240(41.667)	298	220(0.922)	200(0.242)
13	200	220(45.455)	290	200(0.875)	200(0.242)
14	200	220(45.455)	294	200(0.875)	200(0.242)
15	200	220(45.455)	298	220(0.922)	200(0.242)
16	200	200(50)	290	200(0.875)	0
17	200	200(50)	294	200(0.875)	200(0.242)
18	200	200(50)	298	220(0.922)	200(0.242)
19	220	292(34.25)	290	220(0.922)	220(0.201)
20	220	292(34.25)	294	220(0.922)	220(0.201)
21	220	292(34.25)	298	240(0.953)	220(0.201)
22	220	280(35.714)	290	220(0.922)	220(0.201)
23	220	280(35.714)	294	220(0.922)	220(0.201)
24	220	280(35.714)	298	240(0.953)	220(0.201)
25	220	260(38.462)	290	220(0.922)	0
26	220	260(38.462)	294	220(0.922)	220(0.201)
27	220	260(38.462)	298	240(0.953)	220(0.201)
28	220	240(41.667)	290	220(0.922)	0
29	220	240(41.667)	294	220(0.922)	220(0.201)
30	220	240(41.667)	298	240(0.953)	220(0.201)
31	220	220(45.455)	290	220(0.922)	0
32	220	220(45.455)	294	220(0.922)	0
33	220	220(45.455)	298	240(0.953)	0
34	220	200(50)	290	220(0.922)	0
35	220	200(50)	294	220(0.922)	0
36	220	200(50)	298	240(0.953)	0
37	240	292(34.25)	290	240(0.953)	240(0.174)
38	240	292(34.25)	294	240(0.953)	240(0.174)

39	240	292(34.25)	298	260(1.016)	240(0.174)
40	240	280(35.714)	290	240(0.953)	0
41	240	280(35.714)	294	240(0.953)	240(0.174)
42	240	280(35.714)	298	260(1.016)	240(0.174)
43	240	260(38.462)	290	240(0.953)	0
44	240	260(38.462)	294	240(0.953)	240(0.174)
45	240	260(38.462)	298	260(1.016)	240(0.174)
46	240	240(41.667)	290	240(0.953)	0
47	240	240(41.667)	294	240(0.953)	0
48	240	240(41.667)	298	260(1.016)	0
49	240	220(45.455)	290	240(0.953)	0
50	240	220(45.455)	294	240(0.953)	0
51	240	220(45.455)	298	260(1.016)	0
52	240	200(50)	290	240(0.953)	0
53	240	200(50)	294	240(0.953)	0
54	240	200(50)	298	260(1.016)	0
55	260	292(34.25)	290	260(1.016)	260(0.120)
56	260	292(34.25)	294	260(1.016)	260(0.120)
57	260	292(34.25)	298	280(1.102)	260(0.120)
58	260	280(35.714)	290	260(1.016)	0
59	260	280(35.714)	294	260(1.016)	280(0.046)
60	260	280(35.714)	298	280(1.102)	280(0.046)
61	260	260(38.462)	290	260(1.016)	0
62	260	260(38.462)	294	260(1.016)	0
63	260	260(38.462)	298	280(1.102)	0
64	260	240(41.667)	290	260(1.016)	0
65	260	240(41.667)	294	260(1.016)	0
66	260	240(41.667)	298	280(1.102)	0
67	260	220(45.455)	290	260(1.016)	0
68	260	220(45.455)	294	260(1.016)	0
69	260	220(45.455)	298	280(1.102)	0
70	260	200(50)	290	260(1.016)	0
71	260	200(50)	294	260(1.016)	0
72	260	200(50)	298	280(1.102)	0
73	280	292(34.25)	290	280(1.102)	0
74	280	292(34.25)	294	280(1.102)	280(0.046)
75	280	292(34.25)	298	292(1.146)	280(0.046)
76	280	280(35.714)	290	280(1.102)	0
77	280	280(35.714)	294	280(1.102)	0
78	280	280(35.714)	298	292(1.146)	0
79	280	260(38.462)	290	280(1.102)	0
80	280	260(38.462)	294	280(1.102)	0
81	280	260(38.462)	298	292(1.146)	0
82	280	240(41.667)	290	280(1.102)	0
83	280	240(41.667)	294	280(1.102)	0
84	280	240(41.667)	298	292(1.146)	0

85	280	220(45.455)	290	280(1.102)	0
86	280	220(45.455)	294	280(1.102)	0
87	280	220(45.455)	298	292(1.146)	0
88	280	200(50)	290	280(1.102)	0
89	280	200(50)	294	280(1.102)	0
90	280	200(50)	298	292(1.146)	0
91	292	292(34.25)	290	292(1.146)	0
92	292	292(34.25)	294	292(1.146)	292(0.007)
93	292	292(34.25)	298	292(1.146)	292(0.007)
94	292	280(35.714)	290	292(1.146)	0
95	292	280(35.714)	294	292(1.146)	0
96	292	280(35.714)	298	292(1.146)	0
97	292	260(38.462)	290	292(1.146)	0
98	292	260(38.462)	294	292(1.146)	0
99	292	260(38.462)	298	292(1.146)	0
100	292	240(41.667)	290	292(1.146)	0
101	292	240(41.667)	294	292(1.146)	0
102	292	240(41.667)	298	292(1.146)	0
103	292	220(45.455)	290	292(1.146)	0
104	292	220(45.455)	294	292(1.146)	0
105	292	220(45.455)	298	292(1.146)	0
106	292	200(50)	290	292(1.146)	0
107	292	200(50)	294	292(1.146)	0
108	292	200(50)	298	292(1.146)	0
109	294	-	-	294(1.150)	0
110	296	-	-	296(1.148)	0
111	312	-	-	312(1.089)	0
112	332	-	-	332(1.023)	0
113	352	-	-	352(0.965)	0
114	372	-	-	372(0.913)	0
115	392	-	-	392(0.866)	0